Defence Research and Development Canada
Recherche et développement pour la défense Canada

Computational Simulation of Vibrational Overtone Spectral Regions: Sarin

M.W.P. Petryk
DRDC Suffield

Technical Report
DRDC Suffield TR 2006-220
December 2006

Canada

Computational Simulation of Vibrational Overtone Spectral Regions: Sarin

Michael W. P. Petryk
Defence R&D Canada – Suffield

Defence R&D Canada – Suffield

Technical Report

DRDC Suffield TR 2006-220

December 2006

Author

Michael W. P. Petryk

Approved by

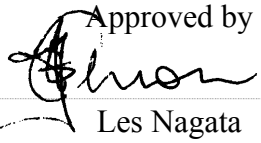

Les Nagata

Head/Chemical Biological Defence Section

Approved for release by

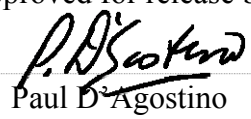

Paul D'Agostino

Head/Document Review Panel

Abstract

In sarin (isopropyl methylphosphonofluoridate) there are ten nonequivalent CH oscillators. *Ab initio* calculations at the HF / 6-311++G(2d,2p) level have been used to determine the vapour phase local mode parameters, $\widetilde{\omega}$ and $\widetilde{\omega}x$, for each oscillator in the two spectrally significant conformers of sarin, as well as inter-oscillator coupling parameters. These above parameters, in conjunction with dipole moment functions derived from *ab initio* calculations, were used to perform harmonically coupled anharmonic oscillator (HCAO) calculations, thereby enabling the simulation of vibrational overtone spectral regions in a room-temperature sample of sarin. It was determined that the computationally-intensive HCAO approach is necessary to predict the lower vibrational overtone regions (*i. e.*, first to third overtones) as a simpler "non-HCAO" approach (which does not allow pairwise harmonic coupling among adjacent oscillators) failed to accurately reproduce the HCAO-simulated spectral regions.

The present work, which was carried out without recourse to the experimental sarin spectral regions, illustrates that it is currently feasible to predict the absorption spectra of species which are difficult to synthesize, handle, or otherwise acquire. In addition to their utility in guiding experimental investigations, the simulated overtone spectral regions will be necessary to correctly assign experimental overtone spectra owing to the large number of similar but nonequivalent CH oscillators present in sarin.

Résumé

Il y a dix oscillateurs CH non équivalents dans le sarin (méthylfluorophosphonate d'isopropyle). Les calculs *Ab initio* au niveau HF / 6-311++G(2d,2p) ont été utilisés pour déterminer les paramètres en mode local de la phase gazeuse, $\widetilde{\omega}$ et $\widetilde{\omega}x$, pour chaque oscillateur dans les deux conformères de sarin spécifiquement signifiants spectralement, ainsi que les paramètres de couplage inter-oscillateurs. Les paramètres ci-dessus, en conjonction avec les fonctions moment dipôle, dérivées des calculs *ab initio*, ont été utilisés pour effectuer des calculs harmoniquement couplés d'oscillateurs non harmoniques (HCAO), permettant ainsi la simulation de régions spectrales ayant une résonance vibrationnelle dans un échantillon de sarin de température ambiante. On a déterminé que la méthode HCAO aux calculs intensifs est nécessaire pour prédire les régions ayant une résonnance vibrationnelle plus basse (par ex. : de la première à la troisième résonnance) parce que la méthode $\ll$non HCAO$\gg$ plus simple (qui ne permet pas le couplage harmonique en paires parmi les oscillateurs adjacents) n'a pas réussi à reproduire avec exactitude les régions spectrales simulées par la HCAO.

Les travaux présents, qui ont été effectués sans avoir recours aux régions spectrales de sarin expérimental, illustrent qu'il est actuellement faisable de prédire le spectre d'absorption des espèces qui sont difficiles à synthétiser, manipuler ou encore acquérir. En plus de leur utilité à guider les investigations expérimentales, les régions spectrales de résonnance simulées seront nécessaires pour assigner correctement le spectre expérimental des résonnances d à la grande quantité d'oscillateurs CH non équivalents présents dans le sarin.

Executive summary

Computational Simulation of Vibrational Overtone Spectral Regions: Sarin

Michael W. P. Petryk; DRDC Suffield TR 2006-220; Defence R&D Canada – Suffield; December 2006.

Background: There is a strong interest in developing the ability to detect chemical threats at a standoff, that is, beyond the effective range of the hazards which these agents pose. The ability to safely interrogate a suspect contaminant at a distance implies the use of some form of spectroscopy, in which light interacts with the threat agent and brings about a change (such as a spectral absorption feature) which can be detected at a distance. Historically, efforts in the standoff detection of chemical warfare agents (CWAs) have focussed on the use of infrared (IR) light in the 2.5–25 μm wavelength region. However, recent advances the telecommunications industry such as the new availability of small, inexpensive, and efficient near-infrared (NIR) diode lasers now encourage further investigations into the possibility of detecting the CWAs spectroscopically in the NIR (*i. e.*, 0.8–25 μm) and visible regions (400–750 nm).

Principal results: It is often desirable to be able to predict, without recourse to any experimental data, the spectral absorption features of CWAs. This is especially important if the CWA in question is difficult to handle, synthesize, or otherwise obtain. In this report it is demonstrated that it is feasible to predict the spectral absorption features of sarin (isopropyl methylphosphonofluoridate) by relying only upon computer models, without any recourse to experimental data. Two computational models have been evaluated in this report, only one of which was found to produce satisfactory results.

Significance of results: This report illustrates that it is feasible to predict (without recourse to the experimental data) the absorption spectra of species which are difficult to synthesize, handle, or otherwise obtain. In addition to their utility in guiding experimental investigations and equipment design, the simulated spectral regions presented herein will be necessary to correctly assign and interpret transitions in the experimental spectral regions.

Future work: Further validation of the approach to spectral simulation reported herein should be undertaken by acquiring the experimental spectral regions of several CWAs in the vapour and liquid phases.

The *ab initio* calculations which were used in the research presented herein were carried out on a publicly-funded academic computer network. It would be advantageous for Defence Research and Development – Suffield to acquire the necessary hardware and software in order to be able to carry out such research in a secure environment.

Sommaire

Computational Simulation of Vibrational Overtone Spectral Regions: Sarin

Michael W. P. Petryk ; DRDC Suffield TR 2006-220 ; R & D pour la défense Canada – Suffield ; décembre 2006.

Contexte : Il y existe un vif intérêt à mettre au point la capacité à détecter des menaces chimiques à distance, c'est à dire au-delà de la portée efficace des menaces que posent ces agents. La capacité à interroger à distance un contaminant suspect en toute sécurité implique l'utilisation d'une forme de spectroscopie dans laquelle la lumière interagit avec l'agent de menace et apporte un changement (tel qu'une caractéristique d'absorption spectrale) pouvant être détectée à distance. Les efforts concernant la détection à distance d'agents de guerre chimiques ont historiquement focalisé sur l'utilisation de la lumière infrarouge (IR) d'une longueur d'onde d'environ 2,5 à 25 μm. Les progrès récents dans le domaine de l'industrie des télécommunications tels que la nouvelle disponibilité de petits lasers à diode proche infrarouge (NIR) économiques et efficaces encouragent cependant maintenant à examiner plus profondément la possibilité de détecter les armes de guerre chimiques spectroscopiquement dans le NIR (par ex. : de 0,8 à 25 μm) et dans des régions visibles (de 400 à 750 nm).

Résultats principaux : Il est souvent désirable d'être en mesure de prédire les caractéristiques d'absorption spectrale d'une arme chimique sans avoir recours à des données expérimentales. Ceci est surtout important si l'arme chimique en question est difficile à manipuler, synthétiser ou obtenir. Ce rapport démontre qu'il est faisable de prédire les caractéristique d'absorption spectrale du sarin (méthylfluorophosphonate d'isopropyle) en se fiant seulement à des modèles informatisés et sans aucun recours à des données expérimentales. Deux modèles de calcul ont été évalués dans ce rapport mais un seul a produit des résultats satisfaisants.

Portée des résultats : Ce rapport illustre qu'il est faisable de prédire le spectre d'absorption des espèces difficiles à synthétiser, manipuler ou obtenir (sans avoir recours à des données expérimentales). En plus de leur utilité à guider les investigations expérimentales et la conception de l'équipement, les régions spectrales simulées mentionnées seront nécessaires pour assigner et interpréter correctement les transitions dans les régions spectrales expérimentales.

Travaux futurs : La validation future de la méthode de simulation spectrale documentée ici devrait être entreprise en acquérant les régions spectrales expérimentales de plusieurs armes chimiques en phase gazeuse et liquide.

Les calculs *ab initio* utilisés dans la recherche présentée ici ont été effectués sur un réseau informatique pédagogique financé par le gouvernement. Il serait avantageux, pour Recherche et développement pour la défense – Suffield, d'acquérir le matériel et les logiciels requis pour effectuer une telle recherche dans un milieu sécuritaire.

Table of contents

List of figures

List of tables

Acknowledgement

This research has been enabled by the use of WestGrid computing resources, which are funded in part by the Canada Foundation for Innovation, Alberta Innovation and Science, B. C. Advanced Education, and the participating research institutions. Specifically, the *ab initio* calculations presented in this report were run on `lattice.westgrid.ca`, which is located at and supported by the University of Calgary.

This page intentionally left blank.

1 Introduction

Vibrational stretching overtone transitions of CH bonds (which occur approximately at frequencies of $n \times 3000$ cm^{-1} where n is an integer which is greater than or equal to two) are potentially exploitable for the portable spectroscopic detection of chemical warfare agents (CWAs) as many such transitions occur in the near-infrared (NIR) and visible regions of the spectrum where small, efficient diode lasers operate. Further, uncooled detectors which operate in the NIR and visible regions are far more sensitive than those which operate in the more commonly exploited fundamental region (*i. e.*, *ca.* 450–3500 cm^{-1}). For example, uncooled indium gallium arsenide (InGaAs) diode detectors operate in the 5800-12500 cm^{-1} region and are approximately six hundred times more sensitive than cryogenically cooled, wide-band mercury cadmium telluride (MCT) detectors which are commonly used in fundamental vibrational spectroscopy and operate in the 420-10000 cm^{-1} region. If cryogenic cooling is impractical or impossible, uncooled deuterated triglycine sulfate (DTGS) detectors are available which operate in approximately the same region as cooled MCT detectors. However, the sensitivities of uncooled DTGS detectors are approximately twenty-five times lower than those of MCT detectors. Unfortunately, vibrational overtone transition intensities decrease rapidly with increasing vibrational excitation such that enhancements realized by increases in portable laser power and detector sensitivities in the lower overtone regions are negated at CH overtones which lie approximately at or above the fourth overtone. This report deals with the computational modelling of vibrational overtone transitions in the nerve agent sarin (isopropyl methylphosphonofluoridate). No attempt is made to propose specific spectroscopic techniques for the detection of vibrational overtone transitions in CWAs as such specific techniques will have to be chosen based upon the intended application (*e. g.*, point detection, standoff detection suitable surveying large areas, *etc.*).

The vibrational overtone stretching transitions of XH bonds (where X = C, N, O, *etc.*) are dominated by transitions into states where all of their vibrational energy is localized within one of a set of equivalent XH bonds. The energy localized within these local modes of vibration [1–5] makes overtone spectroscopy a very sensitive probe for detecting small changes in the properties of XH bonds, such as molecular conformations [6, 7] and bond lengths [8–10].

The molecular Hamiltonian can be expressed in a local mode basis. Such a representation leads to XH stretch terms where off-diagonal coupling elements are small compared to the (anharmonic) diagonal cubic and quartic terms [11]. The contributions of the diagonal terms to the molecular Hamiltonian become increasingly dominant with increasing vibrational excitation. As a result, it is possible to treat the stretching potential of a molecule as a collection of isolated anharmonic oscillators in which inter-oscillator coupling is treated as a perturbation [12]. Often such an-

harmonic oscillators are approximated using Morse oscillators since the energies and matrix elements of the wavefunctions associated with the latter have been solved analytically [4, 13].

If the stretching potential of a molecule is approximated as a collection of isolated (Morse) anharmonic oscillators, the basis states of a molecule comprising n XH Morse oscillators can be written as the product of individual one dimensional Morse wavefunctions $|\upsilon_1\rangle|\upsilon_2\rangle \ldots |\upsilon_i\rangle \ldots |\upsilon_n\rangle$ or simply as $|\upsilon_1, \upsilon_2, \ldots, \upsilon_i, \ldots, \upsilon_n\rangle$, where υ_i is the number of vibrational quanta in the i^{th} oscillator. Those states which carry intensity from the $\upsilon = 0$ ground vibrational state (*i. e.*, spectrally "bright" states), are almost exclusively pure local mode states which are described by a linear combination of components in which all vibrational energy is localized within one oscillator (*e. g.*, $|\upsilon, 0, \ldots, 0\rangle$, $|0, \upsilon, \ldots, 0\rangle$, *etc.*). In the case where the local methyl group has C_1 symmetry (*e. g.*, sarin), the pure local mode wavefunctions of the three uncoupled methyl XH oscillators are denoted $|\upsilon_i\rangle|0\rangle|0\rangle$, $|0\rangle|\upsilon_j\rangle|0\rangle$, and $|0\rangle|0\rangle|\upsilon_k\rangle$. In the case of a CH oscillator, a transition out of the ground state $\upsilon = 0$ into a state excited by n vibrational quanta is often referred to by the change in quanta and denoted $\Delta\upsilon_{\text{CH}} = n$. The local mode description has been extended in the harmonically coupled anharmonic oscillator (HCAO) model [5, 14–17] wherein molecules are treated as a collection of Morse oscillators which are harmonically coupled.

The HCAO model can accurately predict the intensities of light absorption which accompany vibrational overtone transitions, both in terms of the relative absorbance intensities of oscillators within a molecule [18–21], and in terms of the absolute absorbance intensities [22–28]. The HCAO model, used in conjunction with *ab initio* energy and dipole moment calculations, has allowed the accurate prediction of overtone spectra for species which have not been observed experimentally [29, 30]. The transition from normal mode vibrational behaviour to local mode vibrational behaviour (the HCAO model is based upon the latter) in XH stretching oscillators occurs at approximately $\Delta\upsilon_{\text{CH}} = 3$. Simulated CH vibrational overtone spectral regions will be presented for sarin in the $\Delta\upsilon_{\text{CH}} = 3 - 6$ regime.

In sarin there are ten nonequivalent CH oscillators. In this report *ab initio* calculations will be used to determine the local mode parameters, $\widetilde{\omega}$ and $\widetilde{\omega}x$, for each oscillator in all spectrally significant conformers of sarin, as well as inter-oscillator coupling parameters. These above parameters, in conjunction with dipole moment functions derived from *ab initio* calculations, will be used to perform HCAO calculations, enabling the simulation of vibrational overtone spectral regions in a room-temperature sample of sarin.

2 Theory and calculations

2.1 Anharmonic oscillators and local modes of vibration

Vibrational overtone spectra arising from CH stretching transitions can be interpreted within the local mode model of molecular vibration [2,3]. The CH stretching potential is often approximated by a Morse potential [12]

$$V(q) = D_e(1 - \mathrm{e}^{-aq})^2 \tag{1}$$

where D_e is the depth of the potential energy well, a is the Morse scaling factor, and q is displacement from the equilibrium CH bond length. The depth of the potential energy well is given by

$$D_e = \frac{\widetilde{\omega}^2}{4\widetilde{\omega}x} \tag{2}$$

where the terms $\widetilde{\omega}$ and $\widetilde{\omega}x$ are, respectively, the pure local mode frequency and anharmonicity (see below). The Morse scaling factor a is given by

$$a = \frac{\widetilde{\omega}}{\hbar}\sqrt{\frac{\mu}{2D_e}} \tag{3}$$

where μ is the reduced mass of the CH oscillator. The energy eigenvalues, $\widetilde{E}_\upsilon$, of a Morse oscillator can be expressed (in cm^{-1}) by the expression [12, 31]

$$\widetilde{E}_\upsilon = \widetilde{\omega}\left(\upsilon + \frac{1}{2}\right) - \widetilde{\omega}x\left(\upsilon + \frac{1}{2}\right)^2 . \tag{4}$$

This equation can be rearranged to give the frequency of an overtone transition out of the ground state, $\widetilde{\nu}_{\upsilon\leftarrow 0}$, in the form [12]

$$\widetilde{\nu}_{\upsilon\leftarrow 0} = \upsilon\widetilde{\omega} - (\upsilon^2 + \upsilon)\widetilde{\omega}x \ . \tag{5}$$

Experimental values of the Morse parameters $\widetilde{\omega}$ and $\widetilde{\omega}x$ can be obtained either from a Birge–Sponer plot of $\widetilde{\nu}_{\upsilon\leftarrow 0}/\upsilon$ *vs.* υ or from a quadratic fit of $\widetilde{\nu}_{\upsilon\leftarrow 0}$ *vs.* υ. *Ab initio* calculations can also be used to predict local mode parameters [32, 33].

An anharmonic oscillator model for molecular vibrations which neglects coupling between adjacent oscillators (as opposed to the HCAO approach, see Section 2.2), hereinafter referred to as the "non-HCAO" approach, can be used to predict the frequencies of vibrational overtone transitions using *ab initio*-calculated potential energy surfaces (PESs) and equations 1–3 and 5. Such an approach is known to produce systematic errors, overestimating transition frequencies by approximately 10–30 cm^{-1} for lower overtones owing to the neglect of interoscillator coupling (see Section 3.3 for more details). By way of comparison, the magnitude of the error in a typical HCAO-calculated transition frequency is approximately 1–3 cm^{-1}.

2.2 Coupled methyl oscillators

The frequencies of transitions out of the ground $|0\rangle$ state to the excited state $|\upsilon\rangle$ for an isolated CH oscillator are given by equation 5. In the case of coupled CH oscillators on a methyl group with local C_1 symmetry (*e. g.*, sarin), transitions out of the ground $|0\rangle|0\rangle|0\rangle$ state into the states $|\upsilon_i\rangle|0\rangle|0\rangle$, $|0\rangle|\upsilon_j\rangle|0\rangle$, or $|0\rangle|0\rangle|\upsilon_k\rangle$ have an equivalent energy expression, given in terms of the molecular Hamiltonian H, which is [5]

$$\begin{aligned}\frac{H - E_{|0\rangle|0\rangle|0\rangle}}{hc} &= \sum_i^3 \upsilon_i \widetilde{\omega}_i - \sum_i^3 \left(\upsilon_i^2 + \upsilon_i\right) \widetilde{\omega} x_i \\ &- \sum_{i \neq j}^3 \gamma'_{ij} \left(a_i^- a_j^+ + a_i^+ a_j^-\right) \end{aligned} \tag{6}$$

where $E_{|0\rangle|0\rangle|0\rangle}$ is the energy of the vibrational ground state, a^+ and a^- are (respectively) the creation and annihilation operators, and γ'_{ij} is the intramanifold coupling parameter [5]

$$\gamma'_{ij} = (\gamma_{ij} - \phi_{ij}) \sqrt{\widetilde{\omega}_i \widetilde{\omega}_j} \tag{7}$$

where γ_{ij} and ϕ_{ij} are, respectively, the kinetic and potential energy coupling terms. These terms can be expressed as [5]

$$\phi_{ij} = \frac{1}{2} \frac{F_{ij}}{F_{ii} F_{jj}} \tag{8}$$

and

$$\gamma_{ij} = -\frac{1}{2} \frac{G_{ij}}{G_{ii} G_{jj}} \tag{9}$$

where F and G represent the Wilson matrix elements [34]. The diagonal force constants F_{ii} and F_{jj} can be derived from *ab initio* PESs along single stretch coordinates while the non-diagonal force constant F_{ij} can be obtained from *ab initio* PESs along two stretch coordinates [35]. The kinetic energy coupling term γ_{ij} is a function of molecular conformation only and can be expressed as [5]

$$\gamma_{ij} = -\frac{1}{2} \cos(\theta) \left(1 + \frac{m_{\mathrm{C}}}{m_{\mathrm{H}}}\right)^{-1} \tag{10}$$

where m_{C} and m_{H} denote, respectively, the atomic masses of C and H. The value of the H–C–H bond angle θ if often calculated *ab initio*.

2.3 Oscillator strength

Experimental vibrational overtone transition intensities can be expressed in terms of the dimensionless oscillator strength, f_{osc} [36]. By applying the ideal gas law and

using appropriate physical constants [37] an expression for f_{osc} can be obtained in the form

$$f_{\text{osc}} = 2.6935 \times 10^{-9}(\text{Torr m cm})\frac{T}{p\ l}\int A(\tilde{\nu}_{eg})\mathrm{d}(\tilde{\nu}_{eg}) \tag{11}$$

where T is the gas temperature (in Kelvin), p is the pressure of the gas (in Torr), l is the path length (in meters), and $A(\tilde{\nu}_{eg})$ is the absorbance as a function of frequency, $\tilde{\nu}_{eg}$, expressed in wavenumbers (cm^{-1}) for a transition from ground state g to excited state e. The integration is carried out over the frequency range of the absorption feature.

The oscillator strength of an overtone transition can be calculated from the expression [36]

$$f_{\text{osc}} = 4.70175 \times 10^{-7}(\text{cm D}^{-2})\tilde{\nu}_{eg}|\mu_{eg}|^2 \tag{12}$$

where the term 4.70175×10^{-7} denotes a collection of physical constants (taken from Reference [37]), $\tilde{\nu}_{eg}$ denotes the transition frequency (in cm^{-1}), and μ_{eg} is the transition dipole moment matrix element. The transition dipole moment matrix element is given by

$$\mu_{eg} = \langle e|\vec{\mu}|g\rangle \tag{13}$$

where e and g are, respectively, the excited and ground state wavefunctions and $\vec{\mu}$ denotes the dipole moment function (DMF) expressed in Debye (see equation 14, below). The wavefunction of a Morse oscillator excited by υ vibrational quanta can be calculated from the local mode parameters ($\widetilde{\omega}$ and $\widetilde{\omega}x$) and the reduced mass of the oscillator, μ [12].

2.4 The dipole moment function

Within the HCAO model, coupling between adjacent CH oscillators is treated as a pairwise interaction between the oscillator CH_a along internal displacement coordinate q_a and oscillator CH_b along internal displacement coordinate q_b. *Ab initio* calculations are used [18, 19, 38–40] to obtain discrete dipole moment values as functions of q_a and q_b. In this report the dipole moment values are calculated as q_a and q_b are compressed or stretched about their equilibrium CH bond lengths r_e by $\pm$ 0.30 Å in increments of 0.05 Å with all other molecular coordinates constrained to their equilibrium values.[1] The continuous DMF of two coupled oscillators along internal stretch coordinates q_a and q_b is approximated by a Taylor series expansion taken up to sixth order

$$\vec{\mu}(q_a, q_b) = \sum_{i,j=1}^{i+j=6} \vec{\mu}_{ij} q_a^i q_b^j \tag{14}$$

[1]Examples of z-matrices which correspond to the three lowest conformers of sarin are presented in Annex A.

where $\vec{\mu}_{ij}$ are the DMF derivatives

$$\vec{\mu}_{ij} = \frac{1}{i!j!} \frac{\partial^{i+j} \vec{\mu}}{\partial q_a^i \partial q_b^j} \bigg|_{eq} \tag{15}$$

obtained from a fit of *ab initio*-calculated dipole moment values to a polynomial (the subscript *eq* denotes that all other molecular coordinates are constrained to their equilibrium values). Terms in equation 14 include the pairwise mixed derivatives $\partial^2 \vec{\mu}/\partial q_a \partial q_b$, $\partial^3 \vec{\mu}/\partial q_a \partial q_b^2$, and $\partial^3 \vec{\mu}/\partial q_a^2 \partial q_b$. It is important to include terms beyond those which are linear in q since, for example, the second order derivatives $\partial^2 \vec{\mu}/\partial q_a^2$ and $\partial^2 \vec{\mu}/\partial q_b^2$ contribute significantly more to overtone transition intensities than do the linear terms. It is known that "non-HCAO" intensities (where inter-oscillator coupling is neglected) are systematically incorrect [5,14]. The magnitude of the "non-HCAO" intensity errors are such that "non-HCAO" intensities are not presented in this report.

It is known that HCAO calculations better reproduce experimental overtone transition intensities if they use *ab initio* DMFs where computer resources have been spent on larger basis sets rather than on increased levels of electron correlation [41], especially if the molecule does not contain any unsaturated bonds. For transitions to the second vibrational overtone and higher electron correlation effects on the DMF are negligible [22, 41, 42]. In general, it has been found that Hartree-Fock (HF) theory gives excellent DMFs for the purpose of HCAO calculations of CH stretching overtone intensities [22, 41].

2.5 Computational details

Ab initio calculations were carried out using Gaussian 03, Revision C.02 [43] on an HP AlphaServer ES40 cluster with 830 MHz and 670 MHz 64-bit processors. Calculations used all Gaussian defaults save that Gaussian overlay option IOP(3/32=2) was used with all calculations to prevent the possible reduction of the expansion set. All calculations were carried out using SCF=Tight as the 6-311++G(2d,2p) basis set used in this report contains diffuse functions.

For each conformer of interest single point energy calculations were carried out as functions of the CH stretch coordinate q in the displacement range $q \in [-0.30, 0.30]$ Å in steps of 0.05 Å (a total of 13 calculations per unpaired stretch coordinate). In sarin there is one "isolated" (unpaired) CH stretch coordinate and three (coupled) CH stretch coordinates on each of three methyl groups. Within the HCAO model, the methyl CH oscillators give rise to a total of nine (asymmetric) pairwise CH stretch interactions. Thus, for each conformer a total of $13 \times 13 \times 9 + 13 = 1534$ *ab initio* calculations were carried out. The total computation time required for

1534 single point (energy and dipole moment) energy calculations on sarin at the HF / 6-311++G(2d,2p) level of theory and basis set was approximately 43 days of CPU time per processor using the aforementioned hardware. Computation time can be reduced by using several processors in parallel. In the case of "non-HCAO" calculations, only $13 \times 10 = 130$ *ab initio* calculations need be carried out per conformer as pairwise interactions are neglected.

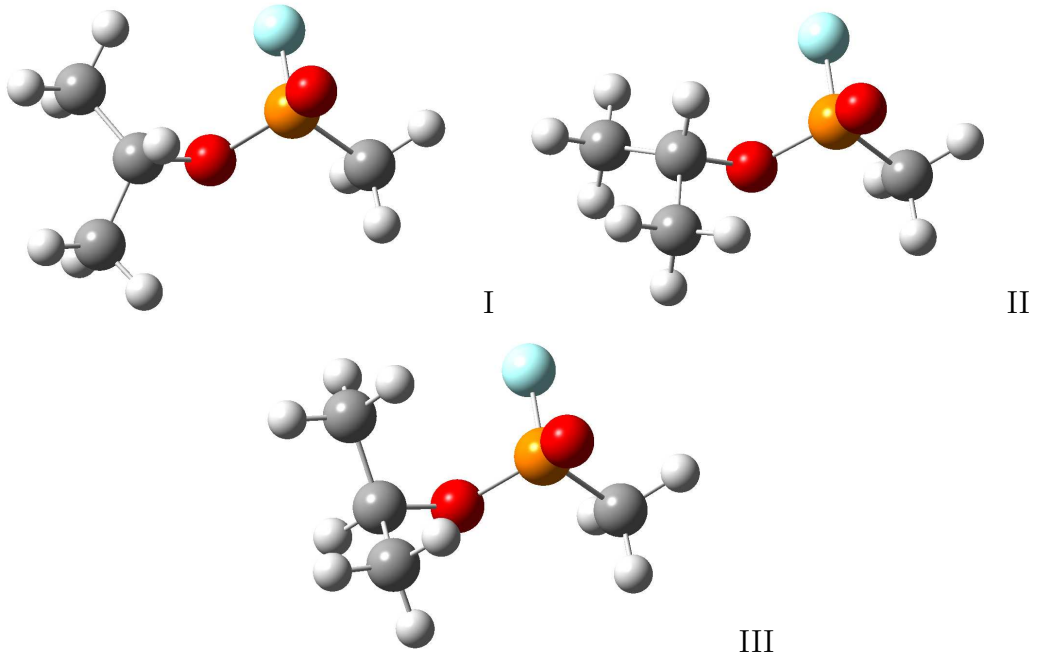

Figure 1: *The vapour phase structures of the three lowest energy conformers of sarin, $(CH_3)_2CHOP(O)(F)CH_3$, calculated at HF / 6-311++G(2d,2p). The* S *enantiomer of sarin is shown. The lowest energy conformer is denoted I, the next lowest energy conformer is denoted II. Conformer III lies significantly higher in energy than conformers I and II (see Table 1).*

3 Results and discussion

3.1 Conformer distributions and geometries

The geometries of the three lowest energy vapour phase conformers of sarin were determined at HF / 6-311++G(2d,2p) and were found to be in agreement with the previous work of Kaczmarek *et al.* [44]. The absences of imaginary frequencies in *ab initio* frequency calculations have confirmed that these three structures represent minima on the PES. These conformers are presented in Figure 1. The lowest energy conformer of sarin is denoted sarin I, the second lowest energy conformer is denoted sarin II, and the subsequent conformer is denoted sarin III.

The methyl group attached to the phosphorous atom in Figure 1 is referred to as $CH_{3,\alpha}$. It contains three CH oscillators which are referred to as CH_1, CH_2, and CH_3. The oscillator which lies approximately in the plane of the page is CH_1. That oscillator which points into the plane of the page is CH_2 while the oscillator which points out of the plane is CH_3. The isopropyl methyl group which is approximately oriented towards the top left-hand side of the page is referred to as $CH_{3,\beta}$ and comprises CH_4,

CH_5, and CH_6. The oscillator CH_4 is that which is oriented towards the upper right-hand side of the page. The CH_5 oscillator is oriented out of the plane of the page while oscillator CH_6 is oriented into the plane of the page. The remaining isopropyl methyl group, $CH_{3,\gamma}$, consists of CH_7, CH_8, and CH_9. The CH_7 oscillator is that which is oriented downwards and into the plane of the page. The orientation of CH_8 is out of the plane of the page and towards the left while oscillator CH_9 is oriented out of the page plane and towards the right-hand side. The isolated CH oscillator which contains the secondary carbon in the isopropyl group is referred to as CH_{10}. There are two oxygen atoms in sarin: O_1 denotes that which is bound to both carbon and phosphorous while O_2 denotes that atom which is bound to phosphorous only. The single geometric parameter which most clearly distinguishes the sarin conformers is the dihedral angle (through the molecular skeleton) between the phosphorous atom and the H atom in CH_{10}, denoted H_{10}. The values of this characteristic angle, $\measuredangle H_{10}$–C–O_1–P, are presented for the S enantiomers of the three sarin conformers in Table 1.

Table 1: *Ab initio-calculated dihedral angles and relative energies of the three lowest energy vapour phase conformers of sarin calculated at HF / 6-311++G(2d,2p)*

	CONFORMER		
PARAMETER	I	II	III
DIHEDRAL ANGLE			
$\measuredangle H_{10}$–C–O_1–P[a]	-28°	18°	168°
RELATIVE ENERGIES[b]			
ΔE	0 cm^{-1}	46.6 cm^{-1}	675 cm^{-1}
ΔE_{ZPVE}	0 cm^{-1}	29.7 cm^{-1}	719 cm^{-1}

[a] This parameter pertains to the S enantiomer of sarin.
[b] Both ZPVE corrected energies, ΔE_{ZPVE}, and non-ZPVE corrected energies, ΔE, are presented.

Previously, van der Waals radii have been used, in conjunction with *ab initio* calculated geometries, as crude metrics to quantify the degree of steric crowding within a molecule [33]. The internuclear separations between hydrogen H_i and an electronegative atom Y (in sarin Y=F or O) to which it is not bound, can be denoted $dH_i \cdots Y$. At internuclear separations $dH_i \cdots Y$ of approximately 2.6 Å or less the separation between atoms H and Y is sufficiently small that nonbonded interactions through space are likely to perturb the vibrational overtone spectrum of a molecule. Such through-space interactions are likely to occur over internuclear separations larger than

approximately 2.6 Å in cases where large amplitude stretching motions (which accompany vibrational overtone transitions) are accompanied by methyl libration [45, 46]. One consequence of through-space coupling is that the initially prepared vibrational stretching overtone state rapidly de-excites *via* intramolecular vibrational energy redistribution (IVR) [12, 47]. The spectral manifestation of IVR is peak broadening caused by lifetime uncertainty, which results in a Lorentzian profile. Based upon the similarity between the internuclear separations $d\mathrm{H}_i \cdots Y$ in sarin [48] and those in the *tert*-butyl halides [33], reasonable full-width at half-maximum (FWHM) estimates for the Lorentzian profiles of the vibrational overtone transitions of sarin are 40 cm^{-1} at $\Delta\upsilon_{\mathrm{CH}} = 3$, 60 cm^{-1} at $\Delta\upsilon_{\mathrm{CH}} = 4$, and 70 cm^{-1} at $\Delta\upsilon_{\mathrm{CH}} = 5, 6$. The HCAO vibrational overtone spectral profiles of sarin have been simulated using slightly smaller FWHM values than those indicated above so as not to obfuscate detail unnecessarily.

The zero-point vibrational energy (ZPVE) corrected energies (at 298.15 K and 1.00 atm pressure) relative to sarin I, ΔE_{ZPVE}, have been calculated at HF / 6-311++G(2d,2p) and are presented in Table 1, along with the non-ZPVE corrected relative energies, ΔE. The ΔE_{ZPVE} value for sarin II was determined to be 29.7 cm^{-1}, which is in good agreement with that reported by Kaczmarek *et al.* [44], who determined the energy difference to be 31.48 cm^{-1} at MP2 / 6-311++G(d,p). The agreement between the sarin III ΔE_{ZPVE} in Table 1 (*i. e.*, 719 cm^{-1}), and that reported by Kaczmarek *et al.* [44] (*i. e.*, 454.68 cm^{-1}) is unexpectedly poor. However, Hight Walker *et al.* [49] reported the sarin III ΔE_{ZPVE} to be 604.5 cm^{-1} at HF / 6-311G(d,p) and 500.8 cm^{-1} at MP2 / 6-311G(d,p). The inclusion of some electron correlation *via* MP2 theory is seen to have had a pronounced effect on the relative energy of the sarin III conformer. The relative energies of the sarin conformers in Table 1 have been used to calculate their relative populations at 298 K in order to scale their relative contributions to the room temperature overtone spectrum of sarin. Based upon their small difference in energy, a nearly racemic mixture of sarin I and II will be present at room temperature. The high relative energy of sarin III is such that this conformer will have a negligible influence and its spectral contributions are neglected in this report.

3.2 Local mode and HCAO parameters

Low barriers to internal methyl rotation (*i. e.*, up to a few tens of wavenumbers) can allow the possibility of hundreds of transitions which contribute to the observed spectral profile [50–52], greatly complicating the observed overtone spectrum. Barriers to internal methyl rotation of *ca.* ≥ 450 cm^{-1} will effectively "lock" a methyl group into a position, breaking the coupling between methyl torsion and CH stretching motions so that free methyl rotation will not complicate observed overtone spectra [53]. The barriers to internal methyl rotation for conformers I and II of sarin have been calculated at HF / 6-311++G(2d,2p) and are presented in Table 2. In sarin I the barriers to internal methyl torsion were 730 cm^{-1} for $\mathrm{CH}_{3,\alpha}$, 1310 cm^{-1} for $\mathrm{CH}_{3,\beta}$,

and 1330 cm^{-1} for $CH_{3,\gamma}$ while those barriers in sarin II were 690 cm^{-1}, 1340 cm^{-1}, and 1370 cm^{-1}, respectively. Visualization of the *ab initio* output indicates that no major skeletal motions have accompanied methyl torsion. These barriers are only approximate: they have not been ZPVE corrected and no scaling factors have been applied. Nevertheless, these barriers are sufficiently high that observed CH stretching overtone spectra will not be complicated by methyl torsion structure. The barrier to internal rotation of the $CH_{3,\alpha}$ methyl group has been previously estimated to be 677.0(4) cm^{-1} [49] from microwave studies at 2 K where only the sarin I conformer should exist in appreciable quantities.

Table 2: *Ab initio barriers to internal methyl rotation (in cm^{-1}) of the two lowest energy conformers of sarin obtained at HF / 6-311++G(2d,2p)*

	METHYL GROUP BARRIER		
CONFORMER	$CH_{3,\alpha}$	$CH_{3,\beta}$	$CH_{3,\gamma}$
I	730	1310	1330
II	690	1340	1370

[a] Barriers have not been ZPVE corrected. No scaling factors have been applied to the values presented in this table.

The overtone transition oscillator strengths (equation 12) were calculated using the transition dipole moments (equation 13) and Morse wavefunctions, which are defined by the vibrational quantum number, υ, and the local mode frequency and anharmonicity, $\widetilde{\omega}$ and $\widetilde{\omega}x$ [12]. The *ab initio* PESs (along the ten CH stretch coordinates in sarin) were calculated at HF / 6-311++G(2d,2p) in CH displacement coordinate $q \in [-0.20, 0.20]$ Å in steps of 0.05 Å. The vapour phase parameters $\widetilde{\omega}$ and $\widetilde{\omega}x$ of sarin I and II were determined from nonlinear fits of the *ab initio* PESs to equation 1 and subsequently scaled by $sf_{\widetilde{\omega}} = 0.9429 \pm 0.0015$ for $\widetilde{\omega}$ and $sf_{\widetilde{\omega}x} = 0.921 \pm 0.015$ for $\widetilde{\omega}x$ [33]. These values of $\widetilde{\omega}$ and $\widetilde{\omega}x$ are presented for the ten CH oscillators of sarin I and II in Table 3.

Table 3: *Ab initio calculated, scaled, vapour phase local mode parameters*[a] $\widetilde{\omega}$ *and* $\widetilde{\omega}x$ *(in* cm^{-1}*) of the two lowest energy conformers of sarin obtained at HF / 6-311++G(2d,2p)*

	CONFORMER			
	I		II	
OSCILLATOR	$\widetilde{\omega}$	$\widetilde{\omega}x$	$\widetilde{\omega}$	$\widetilde{\omega}x$
CH_1	3095 ± 5	58.5 ± 1.0	3098 ± 5	58.3 ± 1.0
CH_2	3102 ± 5	58.4 ± 1.0	3103 ± 5	58.4 ± 1.0
CH_3	3101 ± 5	58.5 ± 1.0	3102 ± 5	58.3 ± 1.0
CH_4	3079 ± 5	59.1 ± 1.0	3077 ± 5	59.4 ± 1.0
CH_5	3066 ± 5	59.3 ± 1.0	3067 ± 5	59.2 ± 1.0
CH_6	3066 ± 5	59.5 ± 1.0	3066 ± 5	59.5 ± 1.0
CH_7	3065 ± 5	59.5 ± 1.0	3061 ± 5	59.5 ± 1.0
CH_8	3068 ± 5	59.2 ± 1.0	3064 ± 5	59.3 ± 1.0
CH_9	3076 ± 5	59.5 ± 1.0	3089 ± 5	58.9 ± 1.0
CH_{10}	3094 ± 5	60.0 ± 1.0	3075 ± 5	60.7 ± 1.0

[a] Local mode parameters have been calculated from a nonlinear fit of *ab initio* data to equation 1 and scaled using the appropriate scaling factors from Reference [33].

The local mode coupling parameters in equation 7 were calculated in a manner identical to that of Kjaergaard *et al.* [35] and are presented in Table 4. The parameter ϕ_{ij} was obtained from an expansion series fit of the CH stretching PES [32,35] calculated *ab initio* in the CH displacement range $q \in [-0.30, 0.30]$ Å in steps of 0.05 Å. The parameter γ_{ij} was calculated using equation 10 and the *ab initio* molecular geometry.

Table 4: *Ab initio calculated local mode coupling parameters*[a] *of the two lowest energy conformers of sarin obtained at HF / 6-311++G(2d,2p)*

	CONFORMER					
	I			II		
OSCILLATORS	ϕ_{ij}	γ_{ij}	γ'_{ij}	ϕ_{ij}	γ_{ij}	γ'_{ij}
CH_1, CH_2	0.00317	0.0132	30.9	0.00314	0.0132	31.2
CH_1, CH_3	0.00339	0.0127	28.8	0.00341	0.0127	28.8
CH_2, CH_3	0.00322	0.0131	30.6	0.00328	0.0130	30.2
CH_4, CH_5	0.00474	0.0123	23.2	0.00474	0.0121	22.6
CH_4, CH_6	0.00481	0.0123	23.1	0.00474	0.0123	23.3
CH_5, CH_6	0.00466	0.0123	23.5	0.00459	0.0124	23.8
CH_7, CH_8	0.00472	0.0123	23.3	0.00466	0.0123	23.5
CH_7, CH_9	0.00456	0.0126	24.7	0.00486	0.0124	23.1
CH_8, CH_9	0.00454	0.0123	23.8	0.00476	0.0122	23.1

[a] Local mode coupling parameters were calculated in a manner identical to that of Kjaergaard *et al.* [35].

3.3 Simulated spectra

Electromagnetic fields select transitions into states where all vibrational energy is localized into one of a set of equivalent XH oscillators. In the case of a methyl group with local C_1 symmetry (*e. g.*, sarin), the dominant overtone transitions will be out of the ground state into states $|\upsilon_i\rangle|0\rangle|0\rangle$, $|0\rangle|\upsilon_j\rangle|0\rangle$, or $|0\rangle|0\rangle|\upsilon_k\rangle$. Such states are referred to as pure local mode states since all vibrational excitation is localized in an individual oscillator. Local mode/local mode combination states of the form $|\upsilon_i - 1\rangle|1\rangle|0\rangle$, $|\upsilon_i - 1\rangle|0\rangle|1\rangle$, *etc.*, can couple into the pure local mode states and steal intensity. At a given vibrational overtone, transitions to pure local mode states occur at lower frequencies than do transitions to local mode/local mode combination states owing to oscillator anharmonicity. The separation in the frequencies of transition to pure local mode states *vs.* transitions to local mode/local mode combination states grows with increasing vibrational excitation, while the intensities of transitions to local mode/local mode combination states decrease (as compared to transitions to pure local mode states) with increasing vibrational excitation. The HCAO-calculated vapour phase vibrational overtone transition frequencies and intensities in the $\Delta\upsilon_{CH} = 3 - 6$ regions are presented in Tables B.1 and B.2 for a Boltzmann-distributed population of sarin I and II at 298 K. Individual HCAO-calculated transitions in the $\Delta\upsilon_{CH} = 3 - 6$ regions appear as vertical lines in, respectively, Figures 2 through 5. The line positions

denote transition frequencies and their heights indicate relative individual intensities. Each individual transition has been assigned a Lorentzian profile with a FWHM appropriate to the degree of vibrational excitation (*i. e.*, 30 cm^{-1} at $\Delta\upsilon_{CH} = 3$, 40 cm^{-1} at $\Delta\upsilon_{CH} = 4$, and 50 cm^{-1} at $\Delta\upsilon_{CH} = 5, 6$) and the individual Lorentzian profiles have been summed to yield HCAO-simulated spectra. It is noteworthy that while the dominant transitions in the $\Delta\upsilon_{CH} = 3-6$ regions are transitions into pure local mode states, combination bands make significant contributions to the observed vibrational spectra, especially at lower overtones (see below).

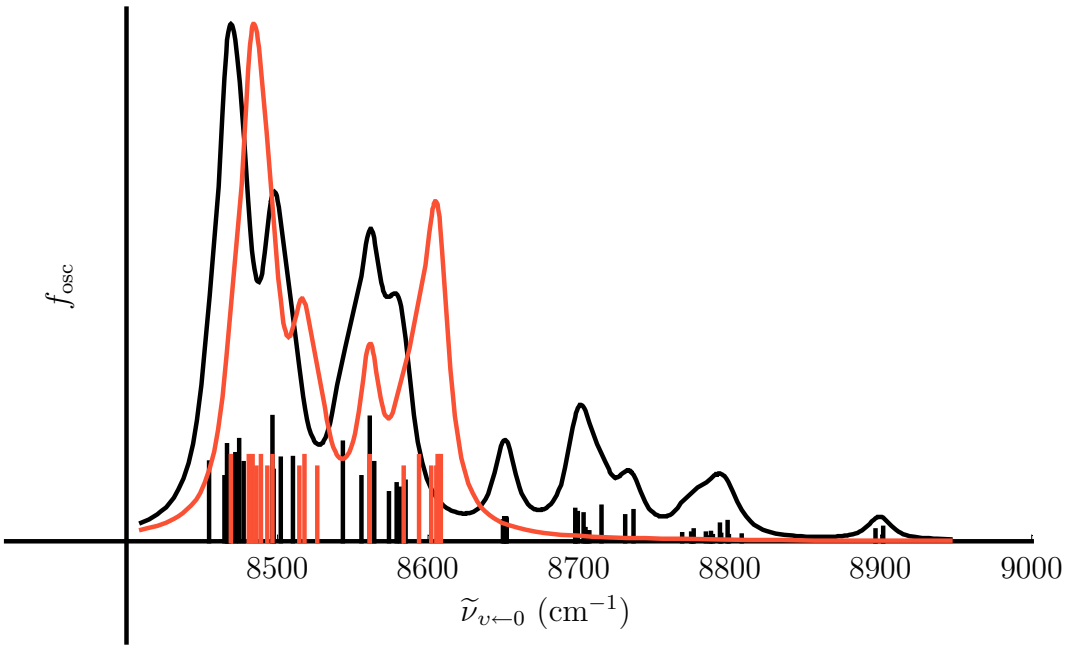

Figure 2: *The vapour phase $\Delta\upsilon_{CH} = 3$ HCAO (black) and "non-HCAO" (red) calculated vibrational overtone spectral region of an equilibrium distribution of sarin I and II conformers at 298 K. The maximum (summed) HCAO absorbance feature in this region has an oscillator strength of 2.47×10^{-9} at ca. 8470 cm^{-1}. The "non-HCAO" trace has been scaled so that its maximum absorbance feature has the same amplitude as the corresponding feature in the HCAO trace.*

Computationally less expensive "non-HCAO" transitions and spectra have been simulated in the $\Delta\upsilon_{CH} = 3 - 6$ regions and are presented in, respectively, Figures 2 through 5. As noted previously, the intensity data from "non-HCAO" calculations are notoriously unreliable—the intensities of the "non-HCAO" transitions have been scaled so that the global maxima of the summed "non-HCAO" spectral profiles are identical to those of the HCAO-calculated profiles. Small variations in the heights of individual "non-HCAO" transition lines reflect the relative abundances of the sarin I and II conformers at 298 K.

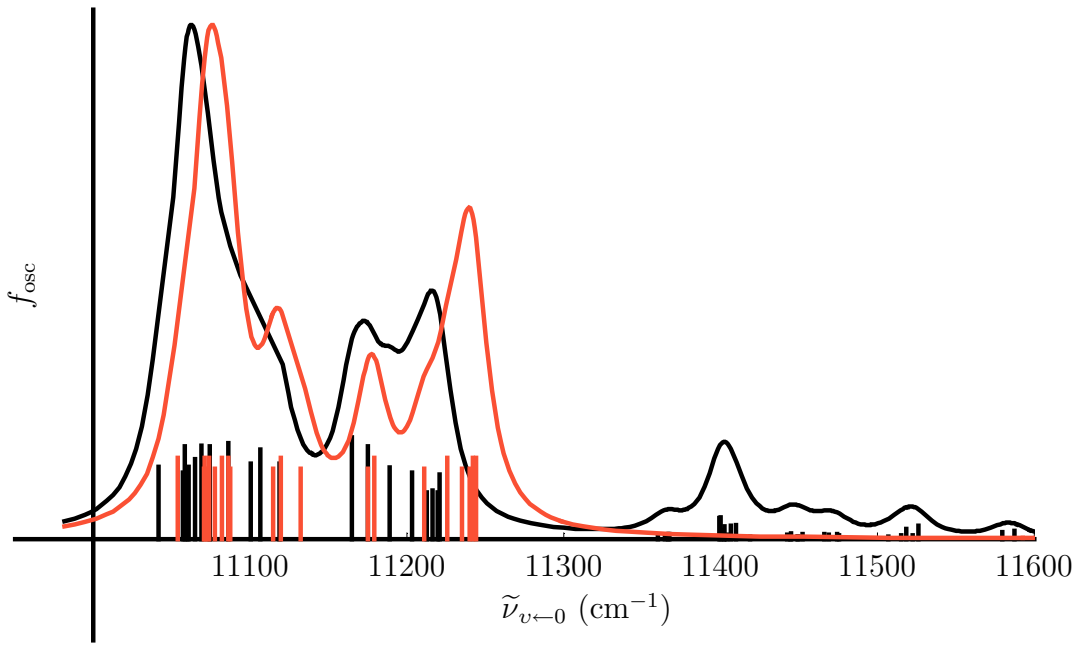

Figure 3: *The vapour phase $\Delta v_{\mathrm{CH}} = 4$ HCAO (black) and "non-HCAO" (red) calculated vibrational overtone spectral region of an equilibrium distribution of sarin I and II conformers at 298 K. The maximum (summed) HCAO absorbance feature in this region has an oscillator strength of 2.56×10^{-10} at ca. 11060 cm^{-1}. The "non-HCAO" trace has been scaled so that its maximum absorbance feature has the same amplitude as the corresponding feature in the HCAO trace.*

The vapour phase HCAO f_{osc} values of the individual Boltzmann weighted transitions within the $v = 3$ manifold are shown in Figure 2 as black vertical lines. The summed HCAO $\Delta v_{\mathrm{CH}} = 3$ profile is shown in black and has a maximum f_{osc} of 2.47×10^{-9} at *ca.* 8470 cm^{-1}. The Boltzmann weighted "non-HCAO" transitions are denoted by red vertical lines. The "non-HCAO" profile is erroneously blue-shifted relative to the HCAO profile as the former neglects interoscillator coupling. However, interoscillator coupling decreases with increasing vibrational excitation [17] so that the disagreement between HCAO and "non-HCAO" transition frequencies will decrease with increasing excitation.

Local mode/local mode combination band structure is absent in the "non-HCAO" profile as the "non-HCAO" approach neglects interoscillator coupling. The presence of significant local mode/local mode combination band structure above *ca.* 8625 cm^{-1} in the HCAO simulation indicates that the accurate calculation of the vibrational overtone spectrum of sarin at $\Delta v_{\mathrm{CH}} = 3$ requires the treatment of inter-oscillator coupling. Agreement between the "non-HCAO" and HCAO calculated spectral regions is poor, indicating that the less expensive "non-HCAO" approach is unsuitable

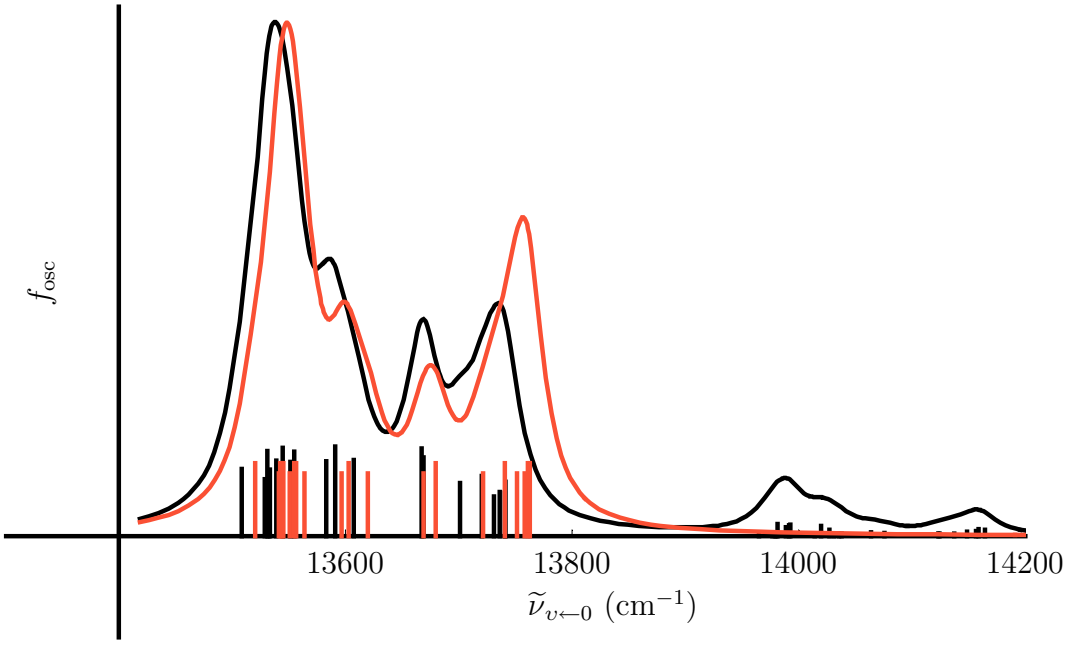

Figure 4: *The vapour phase $\Delta v_{CH} = 5$ HCAO (black) and "non-HCAO" (red) calculated vibrational overtone spectral region of an equilibrium distribution of sarin I and II conformers at 298 K. The maximum (summed) HCAO absorbance feature in this region has an oscillator strength of 2.62×10^{-11} at ca. 13540 cm^{-1}. The "non-HCAO" trace has been scaled so that its maximum absorbance feature has the same amplitude as the corresponding feature in the HCAO trace.*

at $\Delta v_{CH} = 3$.

The simulated HCAO spectral profile at $\Delta v_{CH} = 3$ (and, in fact, at all overtones presented in this report) is deceptively simple as it arises from numerous unresolved CH overtone transitions. Individual vibrational overtone transitions of CH bonds can be resolved from one another in room-temperature vibrational overtone spectra if the bond lengths differ by as little as 1 mÅ [7, 54]. However, in sarin I the CH bond lengths, calculated at HF / 6-311++G(2d,2p), range from 1.079 Å to 1.083 Å, with the difference between the most similar bond lengths[2] being 0.01 mÅ. Similarly, in sarin II, the bond lengths range from 1.080 Å to 1.083 Å with a difference between the most similar bond length values of 0.02 mÅ. A mixture of sarin I and II results in a range of CH bond lengths where the difference between the most similar bond length values is 0.0004 mÅ. The CH vibrational overtone transitions in sarin will not

[2] *Ab initio*-calculated bond length differences on the order of 0.01 mÅ or less are not usually considered to be physically significant as limitations in theory level and basis set are expected to contribute errors which are similar in magnitude for all but the highest level calculations carried out on relatively small molecules.

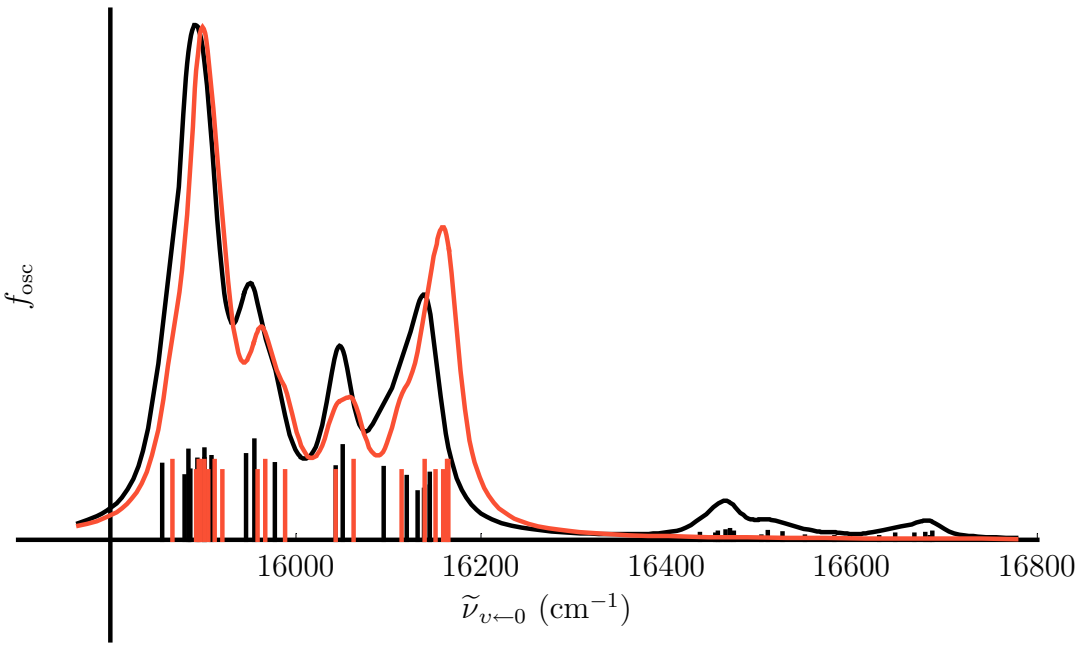

Figure 5: *The vapour phase $\Delta v_{\mathrm{CH}} = 6$ HCAO (black) and "non-HCAO" (red) calculated vibrational overtone spectral region of an equilibrium distribution of sarin I and II conformers at 298 K. The maximum (summed) HCAO absorbance feature in this region has an oscillator strength of 3.42×10^{-12} at ca. 15890 cm^{-1}. The "non-HCAO" trace has been scaled so that its maximum absorbance feature has the same amplitude as the corresponding feature in the HCAO trace.*

be experimentally resolvable at room temperature.

The HCAO and "non-HCAO" $\Delta v_{\mathrm{CH}} = 4$ calculated vapour phase spectral regions are presented in Figure 3 as individual transitions and as summed profiles. The maximum HCAO f_{osc} is 2.56×10^{-10} and occurs at *ca.* 11060 cm^{-1}. Local mode/local mode combination bands are visible above 11350 cm^{-1}. However, these combination bands are less prominent than at $\Delta v_{\mathrm{CH}} = 3$ and are increasingly becoming separated from the pure local mode bands. The numerous unresolved transitions which form the summed HCAO profile reinforce the necessity to carry out HCAO calculations if one is to assign and interpret observed overtone transitions. The disparity between the HCAO profile (which required 1534 *ab initio* calculations per conformer) and "non-HCAO" profile (which required 130 *ab initio* calculations per conformer) indicates that an HCAO approach is required to simulate the $\Delta v_{\mathrm{CH}} = 4$ spectral region of sarin.

The agreement between the HCAO and "non-HCAO" $\Delta v_{\mathrm{CH}} = 5$ simulated vapour phase spectra, presented in Figure 4, is passable. Unfortunately, at this degree of

vibrational excitation (and higher) the inherent intensities of the vibrational overtone transitions are very weak and, in general, are no longer offset by increases in portable laser power and detector efficiency in the visible region of the spectrum. The $\Delta\upsilon_{CH} = 5$ HCAO maximum summed f_{osc} is 2.62×10^{-11} at *ca.* 13540 cm^{-1}. Local mode/local mode combination bands, which occur above 13900 cm^{-1}, are continuing to decrease in significance with increasing vibrational excitation.

The HCAO and "non-HCAO" simulated vapour phase spectra of the $\Delta\upsilon_{CH} = 6$ region are presented in Figure 5. The maximum summed $\Delta\upsilon_{CH} = 6$ HCAO f_{osc} is 3.42×10^{-12} at *ca.* 15890 cm^{-1}. Agreement between the "non-HCAO" and HCAO simulated spectra are adequate for most detection (but not identification) purposes.

4 Conclusions

The three lowest energy vapour phase conformers of sarin have been identified. The two lowest energy conformers were determined to contribute significantly to the spectral profile of a sample of sarin at 289 K. The barriers to internal methyl rotation in sarin were found to be sufficiently high that the coupling of methyl torsion to CH stretching will not complicate the observed overtone spectral regions.

The vapour phase local mode parameters $\widetilde{\omega}$ and $\widetilde{\omega}x$ have been calculated for each of the ten CH oscillators in the two spectrally significant sarin conformers *ab initio* at the HF / 6-311++G(2d,2p) level of theory and basis set, as have the inter-oscillator coupling parameters. In conjunction with dipole moment functions derived from *ab initio* calculations, those parameters above were used to perform harmonically coupled anharmonic oscillator (HCAO) calculations. The HCAO calculations were in turn used to simulate the vapour phase vibrational overtone spectral regions in a room-temperature sample of sarin. It has been shown to be feasible to predict (without recourse to the experimental spectra) the absorption spectra of species which are difficult to synthesize, handle, or otherwise acquire.

The inclusion of inter-oscillator coupling (*via* the HCAO approach) has been shown to be necessary to predict the lower vibrational overtone regions (*i. e.*, first to third overtones) as a simpler "non-HCAO" approach (which does not allow pairwise harmonic coupling among adjacent oscillators) failed to accurately reproduce the HCAO-simulated pure local mode spectral regions.

5 Future work and recommendations

Further validation of the approach to spectral simulation used in this report should be undertaken by acquiring the experimental overtone spectral regions of sarin in the vapour and liquid phases. A comparison of the theoretical and experimental vapour phase spectra will indicate whether Fermi resonances[3] are likely to complicate the overtone spectra of organophosphate nerve agent homologues (*i. e.*, ROP(O)(X)R′), making the task of simulating their vibrational overtone spectra more challenging. Future experimental and theoretical investigations into the vapour phase overtone spectral regions of other nerve agents should be undertaken in order that possibility of deriving local mode scaling factors specific to ROP(O)(X)R′ homologues can be investigated. Finally, the experimental overtone spectra of nerve agents should be acquired in the liquid phase and isolated in matrices so that the effects of solvation on experimental local mode parameters and overtone transition intensities can be compared with results from HCAO calculations based upon *ab initio* solvation models in order to investigate our capability to predict the overtone spectra of CWAs in condensed phases.

The *ab initio* calculations which were used in the research presented in this report were carried out on a publicly-funded academic computer network. It would be advantageous for Defence Research and Development – Suffield to acquire the necessary hardware and software in order to be able to carry out such research in a secure environment.

[3]Energy flow between a pure local mode state and near-resonant combination states has been observed in some molecules. Such an energy flow causes the wavefunctions of the corresponding states to mix. This mixing can be observed as a splitting in the frequency domain [47] which is often referred to as Fermi resonance [55].

References

[1] Mecke, R. and Ziegler, R. (1936), Das Rotationsschwingungsspktrum des Acetylens (C_2H_2), *Z. Phys.*, 101, 405–417.

[2] Hayward, R. J. and Henry, B. R. (1975), A General Local-Mode Theory for High Energy Polyatomic Overtone Spectra and Application to Dichloromethane, *J. Mol. Spectrosc.*, 57, 221–235.

[3] Henry, B. R. (1977), The Use of Local Modes in the Description of Highly Vibrationally Excited Molecules, *Accounts Chem. Res.*, 10, 207–213.

[4] Watson, I. A., Henry, B. R., and Ross, I. G. (1981), Local Mode Behavior: The Morse Oscillator Model, *Spectrochim. Acta A*, 37, 857–865.

[5] Mortensen, O. S., Henry, B. R., and Mohammadi, M. A. (1981), The effects of symmetry within the local mode picture: A reanalysis of the overtone spectra of the dihalomethanes, *J. Chem. Phys.*, 75 (10), 4800–4808.

[6] Swofford, R. L., Long, M. E., and Albrecht, A. C. (1976), C-H vibrational states of benzene, naphthalene, and anthracene in the visible region by thermal lensing spectroscopy and the local mode model, *J. Chem. Phys.*, 65 (1), 179–190.

[7] Henry, B. R. (1987), The Local Mode Model and Overtone Spectra: A Probe of Molecular Structure and Conformation, *Accounts Chem. Res.*, 20, 429–435.

[8] Henry, B. R., Gough, K. M., and Sowa, M. G. (1986), Investigation of CH Bond Lengths and Molecular Conformations, *Int. Rev. Phys. Chem.*, 5, 133–138.

[9] Henry, B. R. and Swanton, D. J. (1989), The Frequency Bond Length Correlation in Local Mode Overtone Spectra, *J. Mol. Struct.*, 202, 193–201.

[10] Kjaergaard, H. G., Proos, R. J., Turnbull, D. M., and Henry, B. R. (1996), CH Stretching Overtone Investigation of Relative CH Bond Lengths in Pyridine, *J. Phys. Chem.*, 100 (50), 19273–19279.

[11] Elert, M. L., Stannard, P. R., and Gelbart, W. M. (1977), Local mode structure of the water molecule, *J. Chem. Phys.*, 67 (11), 5395–5396.

[12] Sage, M. L. and Jortner, J. (1981), Bond Modes, *Adv. Chem. Phys.*, 47, 293–322.

[13] Sage, M. (1978), Morse oscillator transition probabilities for molecular bond modes, *Chem. Phys.*, 35 (3), 375–380.

[14] Child, M. S. and Lawton, T. R. (1981), Local and Normal Vibrational States: a Harmonically Coupled Anharmonic-oscillator Model, *Faraday Discuss. Chem. Soc.*, 71, 273–285.

[15] Henry, B. R., Tarr, A. W., Mortensen, O. S., Murphy, W. F., and Compton, D. A. C. (1983), Raman and Infrared Excitation of Local Modes in Neopentane, *J. Chem. Phys.*, 79 (6), 2583–2589.

[16] Child, M. S. and Halonen, L. (1984), Overtone Frequencies and Intensities in the Local Mode Picture, *Adv. Chem. Phys.*, 57, 1–58.

[17] Henry, B. R. and Kjaergaard, H. G. (2002), Local modes, *Can. J. Chem.*, 80 (12), 1635–1642.

[18] Kjaergaard, H. G., Yu, H., Schattka, B. J., Henry, B. R., and Tarr, A. W. (1990), Intensities in Local Mode Overtone Spectra: Propane, *J. Chem. Phys.*, 93 (9), 6239–6248.

[19] Kjaergaard, H. G., Henry, B. R., and Tarr, A. W. (1991), Intensities in Local Mode Overtone Spectra of Dimethyl Ether and Acetone, *J. Chem. Phys.*, 94, 5844–5854.

[20] Kjaergaard, H. G. and Henry, B. R. (1992), The Relative Intensity Contributions of Axial and Equatorial CH Bonds in the Local Mode Overtone Spectrum of Cyclohexane, *J. Chem. Phys.*, 96, 4841–4851.

[21] Kjaergaard, H. G., Turnbull, D. M., and Henry, B. R. (1993), Intensities of CH and CD-stretching overtones in 1,3-butadiene and 1,3-butadiene-d_6, *J. Chem. Phys.*, 99 (12), 9438–9452.

[22] Kjaergaard, H. G., Daub, C. D., and Henry, B. R. (1997), The Role of Electron Correlation on Calculated XH-Stretching Vibrational Band Intensities, *Mol. Phys.*, 90 (2), 201–213.

[23] Kjaergaard, H. G., Bezar, K. J., and Brooking, K. A. (1999), Calculation of dipole moment functions with density functional theory: application to vibrational band intensities, *Mol. Phys.*, 96 (7), 1125–1138.

[24] Donaldson, D. J., Orlando, J. J., Amann, S., Tyndall, G. S., Proos, R. J., Henry, B. R., and Vaida, V. (1998), Absolute Intensities of Nitric Acid Overtones, *J. Phys. Chem. A*, 102 (27), 5171–5174.

[25] Fono, L., Donaldson, D. J., Proos, R. J., and Henry, B. R. (1999), OH overtone spectra and intensities of pernitric acid, *Chem. Phys. Lett.*, 311 (3–4), 131–138.

[26] Vaida, V., Kjaergaard, H. G., Hintze, P. E., and Donaldson, D. J. (2003), Photolysis of Sulfuric Acid Vapor by Visible Solar Radiation, *Science*, 299, 1566–1568.

[27] Hintze, P. E., Kjaergaard, H. G., Vaida, V., and Burkholder, J. B. (2003), Vibrational and Electronic Spectroscopy of Sulfuric Acid Vapor, *J. Phys. Chem. A*, 107 (8), 1112–1118.

[28] Petryk, M. W. P. and Henry, B. R. (2001), Overtone Intensities in Neopentane and Tetramethylsilane, *Can. J. Chem.*, 79 (3), 279–290.

[29] Sowa, M. G., Henry, B. R., and Mizugai, Y. (1993), Vibrational Overtone Study of 5-Membered Aromatic Heterocycles: Fermi Resonance Interactions, *J. Phys. Chem.*, 97, 809–815.

[30] Low, G. R. and Kjaergaard, H. G. (1999), Calculation of OH-Stretching Band Intensities of the Water Dimer and Trimer, *J. Chem. Phys.*, 110 (18), 9104–9115.

[31] Henry, B. R. (1981), The Local Mode Model, In Durig, J. R., (Ed.), *Vibrational Spectra and Structure*, Vol. 10, pp. 269–319, Amsterdam: Elsevier Scientific.

[32] Sowa, M. G., Henry, B. R., and Mizugai, Y. (1991), Vibrational Overtone Study of 5-Membered Aromatic Heterocycles: Local Mode Interpretations, *J. Phys. Chem.*, 95 (20), 7659–7664.

[33] Petryk, M. W. P. and Henry, B. R. (2005), CH Stretching Vibrational Overtone Spectra Of *tert*-Butylbenzene, *tert*-Butyl Chloride, and *tert*-Butyl Iodide, *J. Phys. Chem. A*, 109 (18), 4081–4091.

[34] Wilson, Jr, E. B., Decius, J. C., and Cross, P. C. (1955), Molecular Vibrations; the Theory of Infrared and Raman Vibrational Spectra, New York: McGraw-Hill.

[35] Kjaergaard, H. G., Henry, B. R., Wei, H., Lefebvre, S., Carrington, Jr, T., and Mortensen, O. S. (1994), Calculation of Vibrational Fundamental and Overtone Band Intensities of H_2O, *J. Chem. Phys.*, 100 (9), 6228–6239.

[36] Atkins, P. W. (1983), Molecular Quantum Mechanics, 2^{nd} ed, Oxford: Oxford University Press.

[37] Cohen, E. R. and Taylor, B. N. (1987), Fundamental Physical Constants, *J. Res. Natl. Bur. Stand.*, 92, 85.

[38] Kjaergaard, H. G. (1992), Local Mode Spectroscopy: Calculation and Measurement of Overtone Intensities, Ph.D. thesis, Odense University, Denmark.

[39] Mortensen, O. S., Ahmed, M. K., Henry, B. R., and Tarr, A. W. (1985), Intensities in Local Mode Overtone Spectra: Dichloromethane and Deuterated Dichloromethane, *J. Chem. Phys.*, 82, 3903–3911.

[40] Tarr, A. W., Swanton, D. J., and Henry, B. R. (1986), SCF Calculations of the CH-Stretching Overtone Intensities in Dichloromethane within the Local Mode Model, *J. Chem. Phys.*, 85, 3463–3468.

[41] Kjaergaard, H. G. and Henry, B. R. (1994), *Ab initio* calcuation of dipole moment functions: application to vibrational band intensities of H_2O, *Mol. Phys.*, 83 (6), 1099–1116.

[42] Daub, C. D., Henry, B. R., Sage, M. L., and Kjaergaard, H. G. (1999), Modeling and Calculation of Dipole Moment Functions for XH Bonds, *Can. J. Chem.*, 77 (11), 1775–1781.

[43] Frisch, M. J., Trucks, G. W., Schlegel, H. B., Scuseria, G. E., Robb, M. A., Cheeseman, J. R., Montgomery, Jr, J. A., Vreven, T., Kudin, K. N., Burant, J. C., Millam, J. M., Iyengar, S. S., Tomasi, J., Barone, V., Mennucci, B., Cossi, M., Scalmani, G., Rega, N., Petersson, G. A., Nakatsuji, H., Hada, M., Ehara, M., Toyota, K., Fukuda, R., Hasegawa, J., Ishida, M., Nakajima, T., Honda, Y., Kitao, O., Nakai, H., Klene, M., Li, X., Knox, J. E., Hratchian, H. P., Cross, J. B., Adamo, C., Jaramillo, J., Gomperts, R., Stratmann, R. E., Yazyev, O., Austin, A. J., Cammi, R., Pomelli, C., Ochterski, J. W., Ayala, P. Y., Morokuma, K., Voth, G. A., Salvador, P., Dannenberg, J. J., Zakrzewski, V. G., Dapprich, S., Daniels, A. D., Strain, M. C., Farkas, O., Malick, D. K., Rabuck, A. D., Raghavachari, K., Foresman, J. B., Ortiz, J. V., Cui, Q., Baboul, A. G., Clifford, S., Cioslowski, J., Stefanov, B. B., Liu, G., Liashenko, A., Piskorz, P., Komaromi, I., Martin, R. L., Fux, D. J., Keith, T., Al-Laham, M. A., Peng, C. Y., Nanayakkara, A., Challacombe, M., Gill, P. M. W., Johnson, B., Chen, W., Wong, M. W., Gonzalez, C., and Pople, J. A. (2004), Gaussian 03, Revision C.02.

[44] Kaczmarek, A., Gorb, L., Sadlej, A. J., and Leszczynski, J. (2004), Sarin and Soman: Structure and Properties, *Struct. Chem.*, 15 (5), 517–525.

[45] Petryk, M. W. P. and Henry, B. R. (2002), Through Space Coupling and Fermi Resonances in Neopentane-d_0, -d_6, -d_9, and Tetramethylsilane, *J. Phys. Chem. A*, 106 (37), 8599–8608.

[46] Petryk, M. W. P., Henry, B. R., and Sage, M. L. (2005), Site–Site Potentials in Neopentane and Tetramethylsilane, *J. Phys. Chem. A*, 109 (44), 9969–9979.

[47] Nesbitt, D. J. and Field, R. W. (1996), Vibrational Energy Flow in Highly Excited Molecules: Role of Intramolecular Vibrational Energy Redistribution, *J. Phys. Chem.*, 100 (31), 12735–12756.

[48] Petryk, M. W. P. (2006), Vibrational Overtone Stretching Transitions in Sarin, (DRDC Suffield SL 2006-067), Defence R&D Canada – Suffield.

[49] Hight Walker, A. R., Suenram, R. D., Samuels, A., Jensen, J., Ellzy, M. W., Lochner, J. M., and Zeroka, D. (2001), Rotational Spectrum of Sarin[1], *J. Mol. Spectrosc.*, 207 (1), 77–82.

[50] Zhu, C., Kjaergaard, H. G., and Henry, B. R. (1997), CH-Stretching Overtone Spectra and Internal Methyl Rotation in 2,6-Difluorotoluene, *J. Chem. Phys.*, 107 (3), 691–701.

[51] Rong, Z., Zhu, C., and Henry, B. R. (2003), CH Stretching Overtone Spectra of Fluorine Substituted Toluenes, *J. Phys. Chem. A*, 107 (49), 10771–10780.

[52] Schofield, D. P. and Kjaergaard, H. G. (2005), Effect of OH internal torsion on the OH-stretching spectrum of *cis,cis*-HOONO, *J. Phys. Chem. A*, 109 (9), 1810–1814.

[53] Rong, Z., Howard, D. L., and Kjaergaard, H. G. (2003), Effect of the methyl internal rotation barrier height on CH-stretching overtone spectra, *J. Phys. Chem. A*, 107 (23), 4607–4611.

[54] Kjaergaard, H. G. and Henry, B. R. (1995), CH Stretching Overtone Spectra and Intensities of Vapor Phase Naphthalene, *J. Phys. Chem.*, 99 (3), 899–904.

[55] Fermi, E. (1931), Raman effect in CO_2, *Z. Phys.*, 71 (46), 250–259.

This page intentionally left blank.

Annex A: *Ab initio* input matrices and geometries

The Gaussian 03 input z-matrices used to calculate the harmonic frequencies of the three lowest energy conformers of sarin are presented below. The parameters which begin with an "r" denote bond lengths (in Å), the parameters which begin with an "a" denote bond angles (in degrees), and the parameters which begin with an "d" denote dihedral angles (in degrees). These parameters are taken from *ab initio* geometry optimizations calculated at HF / 6-311++G(2d,2p) calculated with SCF=Tight and Opt=Tight options specified. Geometry optimizations were run using all Gaussian defaults save that Gaussian overlay option IOP(3/32=2) was used to prevent the possible reduction of the expansion set.

A.1 Sarin conformer I

```
%chk=Ifreq.chk
# HF/6-311++G(2d,2p) Freq SCF=Tight IOP(3/32=2)

Freq (HF/6-311++G(2d,2p)) of conformer I of GB

0 1
P
O1 P rO1P
C2 O1 rC2O P aCOP
C3 C2 rC3C O1 aC3CO P dC3P
C4 C2 rC4C O1 aC4CO C3 dC4C3
H10 C2 rC4H O1 aHCO C3 dHC3
H4 C3 rH4C C2 aH4C O1 dH4O
H5 C3 rH5C C2 aH5C H4 dH5H4
H6 C3 rH6C C2 aH6C H4 dH6H4
H7 C4 rH7C C2 aH7C O1 dH7O
H8 C4 rH8C C2 aH8C H7 dH8H7
H9 C4 rH9C C2 aH9C H7 dH9H7
F P rFP O1 aFO1 C2 dFC2
O2 P rO2P O1 aO2O1 F dO2F
C1 P rC1P O1 aC1O1 F dC1F
H1 C1 rH1C P aH1P F dH1F
H2 C1 rH2C P aH2P H1 dH2H1
H3 C1 rH3C P aH3P H1 dH3H1

rO1P = 1.55219807
```

```
rC2O = 1.44561224
rC3C = 1.51545258
rC4C = 1.5132104
rC4H = 1.07882276
rC1P = 1.78014048
rFP = 1.54526258
rO2P = 1.43778121
rH1C = 1.08069984
rH2C = 1.08005479
rH3C = 1.08023
rH4C = 1.0815011
rH5C = 1.08288668
rH6C = 1.082665
rH7C = 1.08272136
rH8C = 1.08270156
rH9C = 1.0814916
aCOP = 123.8916557
aC3CO = 109.14458558
aC4CO = 106.58583333
aHCO = 107.3419504
aC1O1 = 104.44852
aFO1 = 102.69551244
aO2O1 = 116.30956285
aH1P = 108.81848874
aH2P = 110.35815568
aH3P = 108.96179048
aH4C = 111.07003332
aH5C = 109.75615367
aH6C = 110.60899134
aH7C = 110.67406835
aH8C = 109.8723145
aH9C = 110.62820183
dC3P = 91.12722011
dC4C3 = 122.85968156
dHC3 = -119.29976504
dFC2 = -96.07838913
dO2F = 122.49979869
dC1F = -106.1888713
dH4O = -61.11664106
dH5H4 = -119.57527707
dH6H4 = 120.60261824
dH7O = -61.19614335
```

```
dH8H7 = -119.86383057
dH9H7 = 120.44445118
dH1F = 63.93484782
dH2H1 = -120.6895776
dH3H1 = 118.905770
```

A.2 Sarin conformer II

```
%chk=IIfreq.chk
# HF/6-311++G(2d,2p) Freq SCF=Tight IOP(3/32=2)

Freq (HF/6-311++G(2d,2p)) of conformer II of GB

0 1
P
O1 P rO1P
C2 O1 rC2O P aCOP
C3 C2 rC3C O1 aC3CO P dC3P
C4 C2 rC4C O1 aC4CO C3 dC4C3
H10 C2 rC4H O1 aHCO C3 dHC3
H4 C3 rH4C C2 aH4C O1 dH4O
H5 C3 rH5C C2 aH5C H4 dH5H4
H6 C3 rH6C C2 aH6C H4 dH6H4
H7 C4 rH7C C2 aH7C O1 dH7O
H8 C4 rH8C C2 aH8C H7 dH8H7
H9 C4 rH9C C2 aH9C H7 dH9H7
F P rFP O1 aFO1 C2 dFC2
O2 P rO2P O1 aO2O1 F dO2F
C1 P rC1P O1 aC1O1 F dC1F
H1 C1 rH1C P aH1P F dH1F
H2 C1 rH2C P aH2P H1 dH2H1
H3 C1 rH3C P aH3P H1 dH3H1

rO1P = 1.55209928
rC2O = 1.44687758
rC3C = 1.51356472
rC4C = 1.51379742
rC4H = 1.08005516
rC1P = 1.77979872
rFP = 1.54609944
rO2P = 1.43770942
```

```
rH1C = 1.08071916
rH2C = 1.07995462
rH3C = 1.08023872
rH4C = 1.08146989
rH5C = 1.08282074
rH6C = 1.08264867
rH7C = 1.08302149
rH8C = 1.0830462
rH9C = 1.08064641
aC0P = 122.88457571
aC3C0 = 106.9581287
aC4C0 = 108.45230988
aHC0 = 108.10681882
aC1O1 = 104.24119054
aFO1 = 102.54531762
aO2O1 = 116.52542919
aH1P = 108.75430263
aH2P = 110.39447289
aH3P = 108.96024269
aH4C = 110.69797645
aH5C = 109.89538515
aH6C = 110.56103064
aH7C = 110.45813428
aH8C = 109.89473145
aH9C = 110.44580844
dC3P = 135.99520005
dC4C3 = 123.12764795
dHC3 = -118.26612432
dFC2 = -87.52650936
dO2F = 122.14272659
dC1F = -106.4215882
dH4O = -59.45350453
dH5H4 = -119.84265928
dH6H4 = 120.35992967
dH7O = -60.05386025
dH8H7 = -119.69636064
dH9H7 = 120.66341364
dH1F = 64.38551409
dH2H1 = -120.55506988
dH3H1 = 118.83160012
```

A.3 Sarin conformer III

```
%chk=IIIfreq.chk
# HF/6-311++G(2d,2p) Freq SCF=Tight IOP(3/32=2)

Freq (HF/6-311++G(2d,2p)) of conformer III of GB

0 1
P
O1 P rO1P
C2 O1 rC2O P aCOP
C3 C2 rC3C O1 aC3CO P dC3P
C4 C2 rC4C O1 aC4CO C3 dC4C3
H10 C2 rC4H O1 aHCO C3 dHC3
H7 C3 rH7C C2 aH7C O1 dH7O
H8 C3 rH8C C2 aH8C H7 dH8H7
H9 C3 rH9C C2 aH9C H7 dH9H7
H4 C4 rH4C C2 aH4C O1 dH4O
H5 C4 rH5C C2 aH5C H4 dH5H4
H6 C4 rH6C C2 aH6C H4 dH6H4
F P rFP O1 aFO1 C2 dFC2
O2 P rO2P O1 aO2O1 F dO2F
C1 P rC1P O1 aC1O1 F dC1F
H1 C1 rH1C P aH1P F dH1F
H2 C1 rH2C P aH2P H1 dH2H1
H3 C1 rH3C P aH3P H1 dH3H1

rO1P = 1.55022497
rC2O = 1.44762438
rC3C = 1.51575231
rC4C = 1.51693348
rC4H = 1.07881959
rC1P = 1.78063789
rFP = 1.54576025
rO2P = 1.43810658
rH1C = 1.08074166
rH2C = 1.07991007
rH3C = 1.08029348
rH7C = 1.08213067
rH8C = 1.08325202
rH9C = 1.08008308
rH4C = 1.08150232
```

```
rH5C = 1.08272806
rH6C = 1.08157104
aCOP = 127.93600428
aC3CO = 110.05938518
aC4CO = 111.50018795
aHCO = 102.38426845
aC1O1 = 103.99577746
aFO1 = 102.60792751
aO2O1 = 117.30057445
aH1P = 108.74024546
aH2P = 110.44738668
aH3P = 108.97646918
aH7C = 110.39311746
aH8C = 109.33059246
aH9C = 111.03540767
aH4C = 111.31335865
aH5C = 109.06713619
aH6C = 110.78627298
dC3P = -76.26372773
dC4C3 = 127.28586373
dHC3 = -116.21320077
dFC2 = -92.58859766
dO2F = 122.70973745
dC1F = -106.06245935
dH7O = -53.63459719
dH8H7 = -118.97432431
dH9H7 = 120.85933206
dH4O = -68.05096474
dH5H4 = -119.4588776
dH6H4 = 121.40441189
dH1F = 64.51430506
dH2H1 = -120.57938587
dH3H1 = 118.81112983
```

Annex B: Calculated oscillator strengths

Table B.1: *Transition frequencies (in cm^{-1}), $\widetilde{\nu}_{v\leftarrow 0}$, and oscillator strengths, $f_{\rm osc}$, of the HCAO calculated*[a] *vapour phase CH vibrational overtone transitions $\Delta v = 3-6$ in sarin I*

	$\|CH_1\rangle\|CH_2\rangle\|CH_3\rangle$		$\|CH_4\rangle\|CH_5\rangle\|CH_6\rangle$		$\|CH_7\rangle\|CH_8\rangle\|CH_9\rangle$		$\|CH_{10}\rangle$	
State	$\widetilde{\nu}_{v\leftarrow 0}$	$f_{\rm osc}$	$\widetilde{\nu}_{v\leftarrow 0}$	$f_{\rm osc}$	$\widetilde{\nu}_{v\leftarrow 0}$	$f_{\rm osc}$	$\widetilde{\nu}_{v\leftarrow 0}$	$f_{\rm osc}$
$\|3\rangle\|0\rangle\|0\rangle$	8564	6.99×10^{-10}	8502	7.35×10^{-10}	8455	7.06×10^{-10}		
$\|2\rangle\|1\rangle\|0\rangle$	8794	5.74×10^{-11}	8806	4.63×10^{-12}	8650	2.08×10^{-10}		
$\|1\rangle\|2\rangle\|0\rangle$	8901	1.20×10^{-10}	8705	8.25×10^{-11}	8768	6.61×10^{-11}		
$\|0\rangle\|3\rangle\|0\rangle$	8579	5.07×10^{-10}	8475	9.03×10^{-10}	8467	8.59×10^{-10}		
$\|2\rangle\|0\rangle\|1\rangle$	8798	1.73×10^{-10}	8784	6.86×10^{-11}	8704	1.12×10^{-10}		
$\|0\rangle\|2\rangle\|1\rangle$	8927	7.00×10^{-13}	8776	9.84×10^{-11}	8715	3.10×10^{-10}		
$\|1\rangle\|0\rangle\|2\rangle$	8894	1.39×10^{-11}	8698	2.79×10^{-10}	8799	4.72×10^{-11}		
$\|0\rangle\|1\rangle\|2\rangle$	8736	2.68×10^{-10}	8652	2.08×10^{-10}	8823	1.78×10^{-11}		
$\|0\rangle\|0\rangle\|3\rangle$	8585	5.31×10^{-10}	8468	6.81×10^{-10}	8544	8.79×10^{-10}		
$\Delta v = 3$ total		2.38×10^{-9}		3.07×10^{-9}		3.22×10^{-9}	8497	1.10×10^{-9}
$\|4\rangle\|0\rangle\|0\rangle$	11203	6.20×10^{-11}	11107	8.36×10^{-11}	11042	6.77×10^{-11}		
$\|3\rangle\|1\rangle\|0\rangle$	11474	4.78×10^{-12}	11477	7.54×10^{-13}	11360	3.37×10^{-12}		
$\|1\rangle\|3\rangle\|0\rangle$	11587	7.79×10^{-12}	11402	1.23×10^{-11}	11400	2.04×10^{-11}		
$\|0\rangle\|4\rangle\|0\rangle$	11221	6.02×10^{-11}	11069	8.70×10^{-11}	11058	8.62×10^{-11}		
$\|3\rangle\|0\rangle\|1\rangle$	11523	3.43×10^{-12}	11449	2.58×10^{-12}	11419	2.17×10^{-12}		
$\|0\rangle\|3\rangle\|1\rangle$	11526	1.23×10^{-11}	11367	4.60×10^{-12}	11442	4.24×10^{-12}		
$\|1\rangle\|0\rangle\|3\rangle$	11584	4.81×10^{-13}	11406	1.28×10^{-11}	11469	4.48×10^{-12}		
$\|0\rangle\|1\rangle\|3\rangle$	11618	1.12×10^{-13}	11445	5.48×10^{-12}	11507	2.23×10^{-12}		
$\|0\rangle\|0\rangle\|4\rangle$	11219	4.35×10^{-13}	11061	6.75×10^{-11}	11165	9.45×10^{-11}		
$\Delta v = 4$ total		1.97×10^{-10}		2.79×10^{-10}		2.87×10^{-10}	11086	8.94×10^{-11}
$\|5\rangle\|0\rangle\|0\rangle$	13720	6.27×10^{-12}	13591	9.34×10^{-12}	13508	7.05×10^{-12}		
$\|4\rangle\|1\rangle\|0\rangle$	14137	2.55×10^{-13}	14071	8.10×10^{-14}	13965	3.92×10^{-13}		
$\|1\rangle\|4\rangle\|0\rangle$	14164	6.98×10^{-13}	14039	1.63×10^{-14}	13981	1.29×10^{-12}		
$\|0\rangle\|5\rangle\|0\rangle$	13741	5.69×10^{-12}	13545	9.20×10^{-12}	13531	8.89×10^{-12}		
$\|4\rangle\|0\rangle\|1\rangle$	14206	1.76×10^{-13}	14020	1.13×10^{-12}	14020	1.01×10^{-13}		
$\|0\rangle\|4\rangle\|1\rangle$	14216	1.31×10^{-13}	13991	1.14×10^{-12}	14036	2.75×10^{-13}		
$\|1\rangle\|0\rangle\|4\rangle$	14231	2.80×10^{-14}	14031	2.49×10^{-13}	14076	3.49×10^{-13}		
$\|0\rangle\|1\rangle\|4\rangle$	14159	7.27×10^{-13}	13981	2.70×10^{-13}	14123	2.85×10^{-13}		
$\|0\rangle\|0\rangle\|5\rangle$	13741	4.57×10^{-12}	13533	6.94×10^{-12}	13667	9.19×10^{-12}		
$\Delta v = 5$ total		1.87×10^{-11}		2.85×10^{-11}		2.80×10^{-11}	13554	8.82×10^{-12}
$\|6\rangle\|0\rangle\|0\rangle$	16120	8.62×10^{-13}	15956	1.36×10^{-12}	15856	1.03×10^{-12}		
$\|5\rangle\|1\rangle\|0\rangle$	16728	7.65×10^{-15}	16557	8.08×10^{-15}	16436	7.51×10^{-14}		
$\|1\rangle\|5\rangle\|0\rangle$	16687	9.59×10^{-14}	16517	5.34×10^{-15}	16455	9.49×10^{-14}		
$\|0\rangle\|6\rangle\|0\rangle$	16144	8.98×10^{-13}	15901	1.24×10^{-12}	15884	1.22×10^{-12}		
$\|5\rangle\|0\rangle\|1\rangle$	16667	6.38×10^{-14}	16509	9.76×10^{-14}	16489	1.44×10^{-14}		
$\|0\rangle\|5\rangle\|1\rangle$	16745	7.44×10^{-15}	16468	1.24×10^{-13}	16510	2.19×10^{-14}		
$\|1\rangle\|0\rangle\|5\rangle$	16684	2.85×10^{-14}	16505	2.38×10^{-14}	16581	3.21×10^{-14}		
$\|0\rangle\|1\rangle\|5\rangle$	16749	1.04×10^{-14}	16458	2.81×10^{-14}	16629	2.82×10^{-14}		
$\|0\rangle\|0\rangle\|6\rangle$	16144	7.29×10^{-13}	15886	9.51×10^{-13}	16050	1.28×10^{-12}		
$\Delta v = 6$ total		2.72×10^{-12}		3.85×10^{-12}		3.80×10^{-12}	15901	1.10×10^{-12}

[a] An 11 point grid was used to calculate the dipole moment function derivatives in equation 14.

Table B.2: *Transition frequencies (in cm^{-1}), $\widetilde{\nu}_{\upsilon\leftarrow 0}$, and oscillator strengths, $f_{\rm osc}$, of the HCAO calculated*[a] *vapour phase CH vibrational overtone transitions $\Delta\upsilon = 3-6$ in sarin II*

	$\lvert CH_1\rangle\lvert CH_2\rangle\lvert CH_3\rangle$		$\lvert CH_4\rangle\lvert CH_5\rangle\lvert CH_6\rangle$		$\lvert CH_7\rangle\lvert CH_8\rangle\lvert CH_9\rangle$		$\lvert CH_{10}\rangle$	
State	$\widetilde{\nu}_{\upsilon\leftarrow 0}$	$f_{\rm osc}$	$\widetilde{\nu}_{\upsilon\leftarrow 0}$	$f_{\rm osc}$	$\widetilde{\nu}_{\upsilon\leftarrow 0}$	$f_{\rm osc}$	$\widetilde{\nu}_{\upsilon\leftarrow 0}$	$f_{\rm osc}$
$\lvert 3\rangle\lvert 0\rangle\lvert 0\rangle$	8556	6.62×10^{-10}	8510	8.55×10^{-10}	8465	6.63×10^{-10}		
$\lvert 2\rangle\lvert 1\rangle\lvert 0\rangle$	8789	5.34×10^{-11}	8809	8.83×10^{-12}	8649	2.07×10^{-10}		
$\lvert 1\rangle\lvert 2\rangle\lvert 0\rangle$	8897	1.14×10^{-10}	8699	2.93×10^{-10}	8775	6.02×10^{-11}		
$\lvert 0\rangle\lvert 3\rangle\lvert 0\rangle$	8581	5.42×10^{-10}	8472	8.99×10^{-10}	8478	8.03×10^{-10}		
$\lvert 2\rangle\lvert 0\rangle\lvert 1\rangle$	8994	1.28×10^{-11}	8787	8.58×10^{-10}	8697	1.33×10^{-10}		
$\lvert 0\rangle\lvert 2\rangle\lvert 1\rangle$	8923	2.24×10^{-12}	8774	8.06×10^{-11}	8703	2.79×10^{-10}		
$\lvert 1\rangle\lvert 0\rangle\lvert 2\rangle$	8888	1.77×10^{-11}	8707	9.66×10^{-11}	8786	3.88×10^{-11}		
$\lvert 0\rangle\lvert 1\rangle\lvert 2\rangle$	8793	1.73×10^{-10}	8652	2.28×10^{-10}	8808	5.78×10^{-11}		
$\lvert 0\rangle\lvert 0\rangle\lvert 3\rangle$	8574	4.97×10^{-10}	8467	7.02×10^{-10}	8498	7.29×10^{-10}		
$\Delta\upsilon = 3$ total		2.33×10^{-9}		3.26×10^{-9}		2.99×10^{-9}	8561	1.27×10^{-9}
$\lvert 4\rangle\lvert 0\rangle\lvert 0\rangle$	11189	7.69×10^{-11}	11119	8.15×10^{-11}	11057	7.16×10^{-11}		
$\lvert 3\rangle\lvert 1\rangle\lvert 0\rangle$	11466	5.78×10^{-12}	11482	9.80×10^{-13}	11364	3.99×10^{-12}		
$\lvert 1\rangle\lvert 3\rangle\lvert 0\rangle$	11580	7.64×10^{-12}	11402	1.01×10^{-11}	11399	2.31×10^{-11}		
$\lvert 0\rangle\lvert 4\rangle\lvert 0\rangle$	11216	5.24×10^{-11}	11065	8.59×10^{-11}	11074	9.98×10^{-11}		
$\lvert 3\rangle\lvert 0\rangle\lvert 1\rangle$	11515	4.41×10^{-12}	11452	5.37×10^{-12}	11443	1.33×10^{-12}		
$\lvert 0\rangle\lvert 3\rangle\lvert 1\rangle$	11518	1.10×10^{-11}	11367	5.36×10^{-12}	11449	3.03×10^{-12}		
$\lvert 1\rangle\lvert 0\rangle\lvert 3\rangle$	11576	2.92×10^{-13}	11410	1.50×10^{-11}	11404	5.17×10^{-12}		
$\lvert 0\rangle\lvert 1\rangle\lvert 3\rangle$	11611	2.38×10^{-13}	11445	2.64×10^{-12}	11475	4.44×10^{-12}		
$\lvert 0\rangle\lvert 0\rangle\lvert 4\rangle$	11213	5.02×10^{-11}	11060	7.14×10^{-11}	11100	8.09×10^{-11}		
$\Delta\upsilon = 4$ total		2.11×10^{-10}		2.80×10^{-10}		2.96×10^{-10}	11175	9.98×10^{-11}
$\lvert 5\rangle\lvert 0\rangle\lvert 0\rangle$	13701	6.43×10^{-12}	13607	9.17×10^{-12}	13528	6.86×10^{-12}		
$\lvert 4\rangle\lvert 1\rangle\lvert 0\rangle$	14124	3.58×10^{-13}	14027	8.06×10^{-13}	13977	4.75×10^{-13}		
$\lvert 1\rangle\lvert 4\rangle\lvert 0\rangle$	14157	6.75×10^{-13}	14038	3.63×10^{-13}	13993	1.40×10^{-12}		
$\lvert 0\rangle\lvert 5\rangle\lvert 0\rangle$	13736	5.34×10^{-12}	13539	9.09×10^{-12}	13551	8.96×10^{-12}		
$\lvert 4\rangle\lvert 0\rangle\lvert 1\rangle$	14193	2.12×10^{-13}	14081	8.90×10^{-14}	14028	1.77×10^{-13}		
$\lvert 0\rangle\lvert 4\rangle\lvert 1\rangle$	14207	1.27×10^{-13}	13989	1.11×10^{-12}	14044	8.79×10^{-14}		
$\lvert 1\rangle\lvert 0\rangle\lvert 4\rangle$	14149	5.89×10^{-13}	14035	2.05×10^{-13}	14014	2.92×10^{-13}		
$\lvert 0\rangle\lvert 1\rangle\lvert 4\rangle$	14223	3.48×10^{-14}	13979	3.51×10^{-13}	14064	4.80×10^{-13}		
$\lvert 0\rangle\lvert 0\rangle\lvert 5\rangle$	13731	4.79×10^{-12}	13532	7.07×10^{-12}	13583	9.03×10^{-12}		
$\Delta\upsilon = 5$ total		1.87×10^{-11}		2.84×10^{-11}		2.79×10^{-11}	13669	9.46×10^{-12}
$\lvert 6\rangle\lvert 0\rangle\lvert 0\rangle$	16095	1.13×10^{-12}	15977	1.19×10^{-12}	15880	1.01×10^{-12}		
$\lvert 5\rangle\lvert 1\rangle\lvert 0\rangle$	16709	8.17×10^{-15}	16573	8.88×10^{-15}	16452	8.29×10^{-14}		
$\lvert 1\rangle\lvert 5\rangle\lvert 0\rangle$	16679	8.58×10^{-14}	16512	6.38×10^{-15}	16472	1.06×10^{-13}		
$\lvert 0\rangle\lvert 6\rangle\lvert 0\rangle$	16138	7.84×10^{-13}	15894	1.27×10^{-12}	15909	1.30×10^{-12}		
$\lvert 5\rangle\lvert 0\rangle\lvert 1\rangle$	16647	8.07×10^{-14}	16525	9.57×10^{-14}	16501	1.26×10^{-15}		
$\lvert 0\rangle\lvert 5\rangle\lvert 1\rangle$	16739	1.82×10^{-15}	16463	1.30×10^{-13}	16524	8.22×10^{-15}		
$\lvert 1\rangle\lvert 0\rangle\lvert 5\rangle$	16673	2.18×10^{-14}	16506	1.95×10^{-14}	16502	4.62×10^{-14}		
$\lvert 0\rangle\lvert 1\rangle\lvert 5\rangle$	16736	1.75×10^{-14}	16457	3.00×10^{-14}	16549	4.96×10^{-14}		
$\lvert 0\rangle\lvert 0\rangle\lvert 6\rangle$	16132	7.50×10^{-13}	15885	9.98×10^{-13}	15946	1.34×10^{-12}		
$\Delta\upsilon = 6$ total		2.89×10^{-12}		3.76×10^{-12}		3.95×10^{-12}	16043	1.14×10^{-12}

[a] An 11 point grid was used to calculate the dipole moment function derivatives in equation 14.

DOCUMENT CONTROL DATA

(Security classification of title, body of abstract and indexing annotation must be entered when document is classified)

1. ORIGINATOR (The name and address of the organization preparing the document. Organizations for whom the document was prepared, e.g. Centre sponsoring a contractor's report, or tasking agency, are entered in section 8.)

   Defence R&D Canada – Suffield
   Box 4000, Station Main, Medicine Hat, Alberta,
   Canada T1A 8K6

2. SECURITY CLASSIFICATION (Overall security classification of the document including special warning terms if applicable.)

   UNCLASSIFIED

3. TITLE (The complete document title as indicated on the title page. Its classification should be indicated by the appropriate abbreviation (S, C or U) in parentheses after the title.)

   Computational Simulation of Vibrational Overtone Spectral Regions: Sarin

4. AUTHORS (Last name, followed by initials – ranks, titles, etc. not to be used.)

   Petryk, M.W.P.

5. DATE OF PUBLICATION (Month and year of publication of document.)	6a. NO. OF PAGES (Total containing information. Include Annexes, Appendices, etc.)	6b. NO. OF REFS (Total cited in document.)
December 2006	52	55

7. DESCRIPTIVE NOTES (The category of the document, e.g. technical report, technical note or memorandum. If appropriate, enter the type of report, e.g. interim, progress, summary, annual or final. Give the inclusive dates when a specific reporting period is covered.)

   Technical Report

8. SPONSORING ACTIVITY (The name of the department project office or laboratory sponsoring the research and development – include address.)

   Defence R&D Canada – Suffield
   Box 4000, Station Main, Medicine Hat, Alberta, Canada T1A 8K6

9a. PROJECT NO. (The applicable research and development project number under which the document was written. Please specify whether project or grant.)	9b. GRANT OR CONTRACT NO. (If appropriate, the applicable number under which the document was written.)

10a. ORIGINATOR'S DOCUMENT NUMBER (The official document number by which the document is identified by the originating activity. This number must be unique to this document.)	10b. OTHER DOCUMENT NO(s). (Any other numbers which may be assigned this document either by the originator or by the sponsor.)
DRDC Suffield TR 2006-220	

11. DOCUMENT AVAILABILITY (Any limitations on further dissemination of the document, other than those imposed by security classification.)

   (X) Unlimited distribution
   ( ) Defence departments and defence contractors; further distribution only as approved
   ( ) Defence departments and Canadian defence contractors; further distribution only as approved
   ( ) Government departments and agencies; further distribution only as approved
   ( ) Defence departments; further distribution only as approved
   ( ) Other (please specify):

12. DOCUMENT ANNOUNCEMENT (Any limitation to the bibliographic announcement of this document. This will normally correspond to the Document Availability (11). However, where further distribution (beyond the audience specified in (11)) is possible, a wider announcement audience may be selected.)

   Unlimited

13. ABSTRACT (A brief and factual summary of the document. It may also appear elsewhere in the body of the document itself. It is highly desirable that the abstract of classified documents be unclassified. Each paragraph of the abstract shall begin with an indication of the security classification of the information in the paragraph (unless the document itself is unclassified) represented as (S), (C), (R), or (U). It is not necessary to include here abstracts in both official languages unless the text is bilingual.)

In sarin (isopropyl methylphosphonofluoridate) there are ten nonequivalent CH oscillators. *Ab initio* calculations at the HF / 6-311++G(2d,2p) level have been used to determine the vapour phase local mode parameters, $\widetilde{\omega}$ and $\widetilde{\omega}x$, for each oscillator in the two spectrally significant conformers of sarin, as well as inter-oscillator coupling parameters. These above parameters, in conjunction with dipole moment functions derived from *ab initio* calculations, were used to perform harmonically coupled anharmonic oscillator (HCAO) calculations, thereby enabling the simulation of vibrational overtone spectral regions in a room-temperature sample of sarin. It was determined that the computationally-intensive HCAO approach is necessary to predict the lower vibrational overtone regions (*i. e.*, first to third overtones) as a simpler "non-HCAO" approach (which does not allow pairwise harmonic coupling among adjacent oscillators) failed to accurately reproduce the HCAO-simulated spectral regions.

The present work, which was carried out without recourse to the experimental sarin spectral regions, illustrates that it is currently feasible to predict the absorption spectra of species which are difficult to synthesize, handle, or otherwise acquire. In addition to their utility in guiding experimental investigations, the simulated overtone spectral regions will be necessary to correctly assign experimental overtone spectra owing to the large number of similar but nonequivalent CH oscillators present in sarin.

14. KEYWORDS, DESCRIPTORS or IDENTIFIERS (Technically meaningful terms or short phrases that characterize a document and could be helpful in cataloguing the document. They should be selected so that no security classification is required. Identifiers, such as equipment model designation, trade name, military project code name, geographic location may also be included. If possible keywords should be selected from a published thesaurus. e.g. Thesaurus of Engineering and Scientific Terms (TEST) and that thesaurus identified. If it is not possible to select indexing terms which are Unclassified, the classification of each should be indicated as with the title.)

local mode, overtone transition, Fermi resonance, coupling, scaling factor, normal mode, ab initio, calculated frequencies, vibrational mode, molecular vibration